J. Math. Biol. 42: 195–238 (2001)
Digital Object Identifier (DOI):
10.1007/s002850000037

Mathematical Biology

Howard A. Levine · Brian D. Sleeman · Marit Nilsen-Hamilton

Mathematical modeling of the onset of capillary formation initiating angiogenesis

Received: 27 May 1999 / Revised version: 28 December 1999 /
Published online: 16 February 2001 –

Abstract. It is well accepted that neo-vascular formation can be divided into three main stages (which may be overlapping): (1) changes within the existing vessel, (2) formation of a new channel, (3) maturation of the new vessel.

In this paper we present a new approach to angiogenesis, based on the theory of reinforced random walks, coupled with a Michaelis-Menten type mechanism which views the endothelial cell receptors as the catalyst for transforming angiogenic factor into proteolytic enzyme in order to model the first stage. In this model, a single layer of endothelial cells is separated by a vascular wall from an extracellular tissue matrix. A coupled system of ordinary and partial differential equations is derived which, in the presence of an angiogenic agent, predicts the aggregation of the endothelial cells and the collapse of the vascular lamina, opening a passage into the extracellular matrix. We refer to this as the onset of vascular sprouting. Some biological evidence for the correctness of our model is indicated by the formation of teats in utero. Further evidence for the correctness of the model is given by its prediction that endothelial cells will line the nascent capillary at the onset of capillary angiogenesis.

1. Introduction

An understanding of the mechanisms of capillary sprout formation as a result of endothelial cell migration is fundamental to the understanding of vascularization in many physiological and pathological situations. For example, evidence that most

H.A. Levine: Department of Mathematics, Iowa State University, Ames, IA, 50011, USA. e-mail: halevine@iastate.edu

B.D. Sleeman: School of Mathematics, University of Leeds, Leeds LS2 9JT, England, UK. e-mail: bds@amsta.leeds.ac.uk

M. Nilsen-Hamilton: Department of Biochemistry, Biophysics and Molecular Biology, Iowa State University, Ames, Iowa, 50011,USA. e-mail: marit@iastate.edu

The first two authors were supported in part by NATO grant CRG-95120 and in part by NSF grant DMS-98-03992. The authors also thank Professor Stephen Ford of the Department of Animal Sciences of Iowa State, Dr. Pam Jones of St. James University Hospital, Leeds and Dr. Bryan Dixon of Cookridge Hospital, Leeds for for several stimulating discussions and enlightening comments.

The authors thank Professor Karl Rakusan and the New York Academy of Sciences for permsission to use the figures from [46].

Key words: Angiogenesis – Capillary formation – Growth factors – Reinforced random walk – Michealis-Menten kinetics

capillary growth in the rat heart takes place in the early stages of post natal development [44, 50] was followed by the findings of concomitant changes in the expression of various growth factors [15, 17]. However this interaction is not fully understood; particularly in the study of endothelial cell growth. There is well documented evidence that results from "in vitro" studies cannot be automatically extrapolated to the situation "in vivo". Indeed transforming growth factor β (TGFβ) which suppresses the proliferation of endothelial cells in vitro has an overall angiogenic effect in vivo [50].

Capillaries are remarkably stable structures. For example, the turnover of endothelial cells in the adult mammalian heart is probably slightly faster than in most other tissues. Nevertheless the cell half-life is estimated to be approximately 300 days [24]. Most of the formation of new vascular material normally constitutes replacement of damaged cells and re-population of denuded areas in pathological processes such as wound healing.

However, in the development of tumors, capillary growth through angiogenesis leads to vascularization of the tumor, providing it with its own blood supply and consequently allowing for rapid growth and meta-stasis.

It is important to distinguish the main features of vascularization; that is vasculogenesis and angiogenesis. Vasculogenesis is defined as the formation of new vessels in sites from pluripotent mesenchymal cells (e.g. angioblasts) whereas angiogenesis is defined as the outgrowth of new vessels from a pre-existing network. We shall be concerned with angiogenesis. Both vasculogenesis and angiogenesis have been documented during prenatal development of mammalian hearts [24, 42, 44]. For example in the case of the rat heart, up to day 10 post-fertilization the endocardium is smooth, and the only mode of oxygen transport is by diffusion. This is followed by vasculogenesis initiating from sinusoids lined by a very thin endothelium which are located within the spongious myocardium. Angiogenesis follows in the form of sprouts emanating from the branches of coronary arteries, starting in the subepicardial layer and proceeding towards the sinuses located in the endomycardium. The newly formed vessels may subsequently regress or persist as capillaries or they may progress to form larger vessels of arterial or venous type.

Vascular growth is a complex phenomena involving the mechanisms of angiogenesis. These include mechanical factors in which there is an increased red blood cell (erythrocyte) – endothelial interaction, as in polycythemia, an increased wall tension as a result of increased capillary pressure and an increased shear stress resulting from increased velocity flow. Energy imbalance due to hypoxia may be another major factor in triggering angiogenesis. Inflammatory processes may also be associated with the activation of endothelial cells and possibly platelets; both of which express adhesion molecules for monocytes. Monocytes are a possible major source of angiogenic growth factors. For a discussion of these issues we refer the reader to [1, 7, 23, 49].

Another important aspect of vascular growth is the influence of various growth factors, [19, 26, 27]. The effects vary depending on the environment, the concentrations and combinations of these factors and the cell types involved.

The most often cited angiogenic peptides that are effective both in vivo and in vitro are acidic and basic fibroblast growth factors (FGFs), vascular endothe-

lial growth factor (VEGF), transforming growth factor alpha (TGFα) and related epidermal growth factor (EGF).

The factors VEGF and PD-ECGF (platelet-derived endothelial cell growth factor) are mitogenic factors highly specific for endothelial cells. VEGF may be induced by hypoxia. The fibroblast growth factors are potent mitogens and angiogenesis factors that are released by cells in instances of tissue damage such as occurs on wounding.

In addition to these factors that are endothelial cell mitogens, there are angiogenic factors which are not mitogenic or are even inhibitory to endothelial cell proliferation in vitro. For example these include transforming growth factor beta (TGFβ) and tumor necrosis factor alpha (TNFα).

Vascular growth can also be modified and regulated by local geometric conditions; endothelial cell size and shape and influences from other nearby cell types such as smooth muscle cells, pericytes, platelets, macrophages and mast cells. Macrophages and activated platelets are also important and sometimes major sources of angiogenic factors involved in all stages of vessel formation. [9, 49, 57].

The complexity of the endothelial growth process and the large number of apparently redundant angiogenic factors may be an indication [26] of the vital importance of the process itself. Indeed the fine tuning and interaction of the above systems maintains this delicate balance for the optimal arrangement of vascular geometry.

At the present time it appears to be a formidable task to develop a complete mathematical model of angiogenesis which incorporates all of the above complex processes. It is desirable nevertheless to attempt to describe a portion of this process. This paper therefore concentrates on the importance of some of the angiogenic factors involved. In particular it focuses on the angiogenic factors associated with the neovascular phase of solid tumor growth.

To this end we first discuss the major morphological components of the stable vessel that are potentially involved in the process of angiogenesis. The most prominent are the flat endothelial cells themselves. Typically one or two endothelial cells are required to encircle the capillary lumen. These cells are not to be regarded as simply a passive lining of the micro-vessels, but rather as a composite in a large and extremely active endocrine organ. The capillary as a whole is wrapped in a basement membrane which is only a fraction of the thickness of the endothelial cells. The basement membrane also covers infrequently occurring pericytes which are similar to smooth muscle cells. Pericytes possibly contribute to the regularization of the vessel size and control the proliferation of endothelial cells. This regulation requires cell-to-cell contact – and may also be mediated in part by TGFβ, which suppresses endothelial cell proliferation associated with the inhibition of the neovascular phase of solid tumor growth.

It is now well accepted, [43, 7], that vascular neoformation can be divided into three main stages (which may be overlapping):

1. changes within the existing vessel;
2. formation of a new channel;
3. maturation of the new vessel.

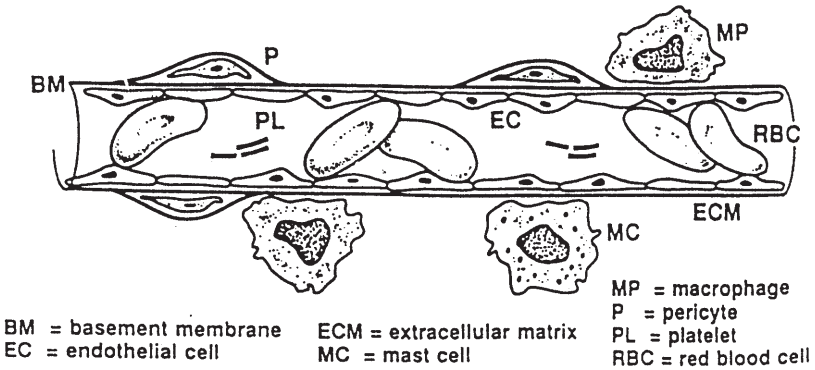

Fig. 1. Sequential steps for vascular growth [46]. Normal capillary.

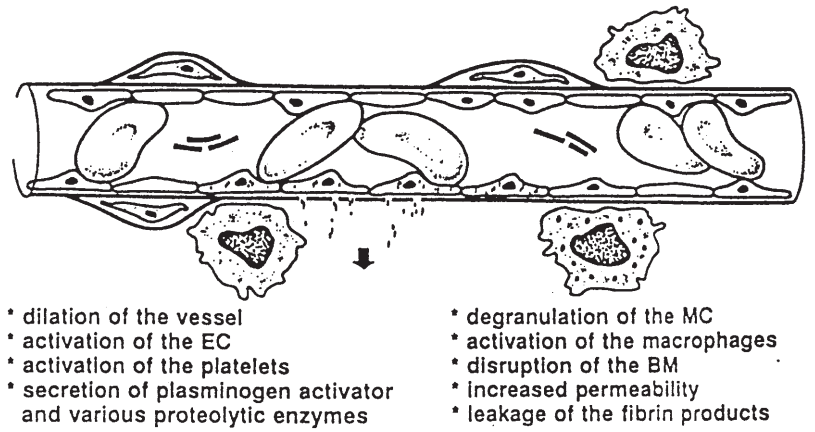

Fig. 2. Sequential steps for vascular growth [46]. Onset of angiogenesis.

The entire process of angiogenesis is discussed elegantly in [18,29,46]. Figure 1 of [18] contains a nice overall view of the process. Figure 1 of [29] provides an illustration of several biochemical pathways, one which we invoke here. Figures 1–4 which are taken from [46] illustrate the events in stage 1. This paper concentrates on stage 1, while the modeling of stages 2 and 3 will be the subjects of further work.

In tumor angiogenesis, stages 2 and 3 have been actively studied over the past decade by a number of workers, see for example, [2,11,24,43,45,53,54] and the references cited therein. In these works emphasis has mostly been centered on modeling capillary development initiating from pre-existing sprout (or buds) from the capillary lumen. In other words, stage 1 (Fig. 2) is assumed to be already activated. Nevertheless, as mentioned above, the main stages may overlap and it will be seen that the ideas developed here reinforce some of the above results. The approach to the modeling problem we use here is quite different. We model the problem at

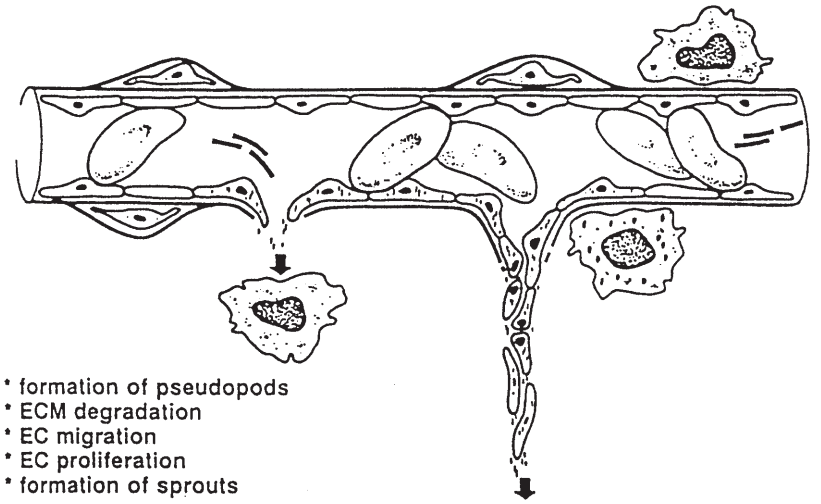

Fig. 3. Sequential steps for vascular growth [46]. Channel formation.

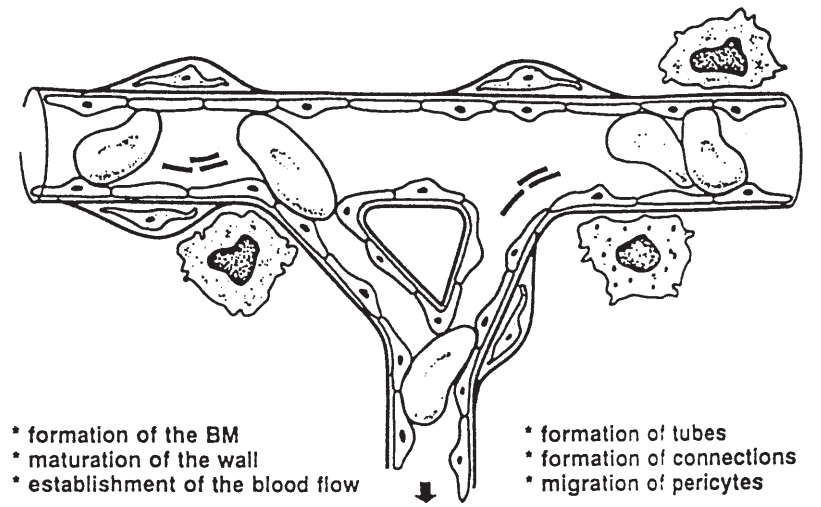

Fig. 4. Sequential steps for vascular growth [46]. Notice the anastomosis (capillary loop).

the molecular and cellular levels using enzyme kinetics coupled with the notion of reinforced random walks. To our knowledge, the application of reinforced random walks to model angiogenesis is completely new although other variants of chemotactic transport have been used in the past.

In stage 1 one of the primary events is the dilation of the vessel. This is followed by the activation of the endothelial cells which in concert with their stretching show an increased sensitivity to various growth factors. The endothelial cells respond by secreting plasminogen activator and a variety of proteolytic enzymes that degrade

the extra-cellular matrix where growth factors such as FGF and at least one form of VEGF are stored.

Subsequently the basement membrane becomes disrupted and local extravasation takes place. Leaked fibrinogen and fibronectin products serve as a provisional matrix for future growth. Also, the activated endothelial cells start to synthesis new DNA while they are still in the parent vessel. Additional growth factors are provided by nearby activated platelets and macrophages.

In regard to tumor growth, angiogenesis is initiated by the release of angiogenic factors from the tumor or surrounding cells. In response to this stimulus, activated endothelial cells in nearby capillaries appear to thicken and finger-like protrusions can be observed on the abluminal surface [5, 43]. Cell-associated proteases degrade the basement membrane allowing the endothelial cells (EC's) to accumulate in the region where the concentrations of TAF (tumor angiogenic growth factor) reaches a threshold [43]. The vessel wall dilates as the EC's aggregate, i.e. accumulate, to form sprouts. More precisely, the EC's, as described above, release proteolytic enzymes which degrade the basal lamina and extracellular matrix (ECM) enabling the capillary sprouts to migrate towards the tumor [25].

With this motivating background we now focus on the development of mathematical models of the first stage of angiogenesis. The plan of this paper is as follows:

In Section 2, we develop the mathematical models. In Section 2.1, each endothelial cell is considered to be sensitive to the angiogenic factor via a Michaelis-Menten type reaction in which angiogenic factor first binds to a receptor on the surface of the endothelial cell. The receptor is then activated and initiates a series of events that result in the production and release of proteases. The proteases break down the ECM and basement lamina. This permits the eventual migration of the endothelial cells toward the tumor proteolytic degradation of the ECM also results in the release of growth factors that stimulate migration and proliferation of the EC.

In Section 2.2, the movement of endothelial cells is modeled using the idea of reinforced random walks. The core of the idea is that the accumulation of endothelial cells in a localized neighborhood along a capillary is stimulated by (1) a large concentration of protease in that neighborhood and (2) low levels of fibronectin, representing the ECM in general, in that neighborhood. We expect therefore, that sprouting should occur along the lamina where the concentration of growth factor is large since it is there where protease production will be larger and fibronectin density will consequently be smaller.

The explicit solvability of the system derived in Section 2 is not feasible. Moreover, a detailed mathematical analysis of the model may not be appealing to all readers. Therefore, in an Appendix, (Section 7) we carry out a preliminary analytical investigation of our model based primarily on our work in [31] which, in its turn, was an analytic study of the equations for reinforced random walks of the type considered numerically in [41]. In these sections, we discuss the ill-posed nature of the model. (Here the term "ill-posed" is taken in the technical sense, a problem for which one of existence, uniqueness or continuous data dependence fails.) Our

contention here is that the ill posed nature of the system provides the mathematical explanation for the onset of angiogenesis.

In Section 3, we present the data for a number of numerical experiments. We discuss the sensitivity of the model to changes in initial data and in the parameters involved in the model. In Section 4, we comment on the numerical results and their sensitivities to step sizes. The biological implications of our investigations are discussed in Section 5 we describe the results of our experiments. We conclude with a discussion of current and future research in Section 6.

The paper concludes with a brief discussion of current research directions.

2. Mathematical models

A mathematical model describing the onset of capillary sprouts in tumor angiogenesis has been developed in [39]. In this model the authors concentrated on the role of haptotaxis to regulate all movement due to the release of fibronectin which increases cell-to-matrix adhesiveness and also serves as a provisional matrix for future growth. The model is based on reaction-diffusion mechanisms and capillary sprout formation is accounted for through Turing diffusion driven instability [34, 58].

Here a different point of view is offered, based on the idea of reinforced random walks [13]. This idea was developed and exploited in [41] to describe the movement of living organisms that deposit a non-diffusible substance (signal) which modifies the local environment for subsequent movement. The particular organisms studied are the myxo bacteria particularly myxococus fulvius and the myxamoebae dictyostelium discoidium. In the continuum limit Othmer and Stevens [41] derive a system of evolutionary equations which may exhibit finite-time blow up of solutions, decay to a spatially constant solution, or non-constant, piecewise constant solutions (aggregation). In [31] the authors have provided detailed rigorous and semi-rigorous arguments which support the existence of aggregation.

Aggregation, that is, endothelial cell accumulation, as mentioned above, is an important component in the initiation of sprout formation. Following activation, cell-released proteases degrade the basal lamina (BL) adjacent to the the activated EC. The EC loosen their contact with their neighbors and begin to penetrate the BL. The wall of the capillary bulges and a small sprout is formed. This sprout is composed of EC where the angiogenic stimulus has reached a threshold (p 202 of [43]).

In the next section we discuss the enzyme kinetics we wish to employ in our model. In the subsequent section, we apply the ideas of random walk discussed above to the vascular wall.

2.1. Enzyme kinetics

In order to better understand how the angiogenic factor acts on endothelial cells we consider that each cell has a certain number of receptors to which the angiogenic factors (ligands) bind. The receptor-ligand complexes (intermediates) in turn stimulate the cell to produce proteolytic enzymes and form new receptors.

We propose to model this process in the following manner:

If V denotes a molecule of angiogenic factor (substrate) and R denotes some receptor site on the endothelial cell wall, they combine to produce an intermediate complex, RV which is an activated state of the receptor that results in the production and secretion of proteolytic enzyme, C, and a modified intermediate receptor R'. The receptor R' is subsequently removed from the cell surface after which it is either recycled to form R or a new R is then synthesized by the cell. It then moves to the cell surface.

Finally the proteolytic enzyme, C degrades the laminar wall leaving a product F' by acting as a catalyst for fibronectin degradation. The products F' need not concern us here. We use classical Michealis-Menten kinetics for this standard catalytic reaction.

The point of view is that the receptors at the surface of the cell function the same way an enzyme functions in classical enzymatic catalysis. In symbols,

$$\begin{aligned} V + R &\underset{k_{-1}}{\overset{k_1}{\rightleftharpoons}} RV \\ RV &\overset{k_2}{\to} C + R' \\ R' &\overset{k_2'}{\to} R \end{aligned} \tag{2.1.1}$$

$$\begin{aligned} C + F &\overset{k_3}{\to} \left[CF\right] \\ \left[CF\right] &\overset{k_4}{\to} F' + C \end{aligned} \tag{2.1.2}$$

We simplify the above chemical mechanism by combining steps (2) and (3) in the above mechanism as follows:

$$V + R \underset{k_{-1}}{\overset{k_1}{\rightleftharpoons}} RV \tag{2.1.3}$$

$$\begin{aligned} RV &\overset{k_2}{\to} C + R \\ C + F &\overset{k_3}{\to} \left[CF\right] \\ \left[CF\right] &\overset{k_4}{\to} F' + C \end{aligned} \tag{2.1.4}$$

Let x denote position along the capillary vessel wall and t denote the time. With concentration expressed in micro moles per unit liter (micro molarity), we define the following quantities:

$$\begin{aligned} v &= \text{concentration of angiogenic factor, } V \\ c &= \text{concentration of proteolytic enzyme, } C \\ r &= \text{density of receptors on the cell directed into the basement lamina, } R \end{aligned} \tag{2.1.5}$$

ℓ = concentration of intermediate receptor complex, RV

η = concentration of endothelial cells

f = density of fibronectin

Applying the law of mass action to the first two equations in (2.1.3) we obtain:

$$\begin{aligned}
\frac{\partial r}{\partial t} &= -k_1 r v + (k_{-1} + k_2)\ell \\
\frac{\partial \ell}{\partial t} &= k_1 r v - (k_{-1} + k_2)\ell \\
\frac{\partial v}{\partial t} &= -k_1 r v + k_{-1}\ell \\
\frac{\partial c}{\partial t} &= k_2 \ell.
\end{aligned} \tag{2.1.6}$$

Applying standard Michealis-Menten kinetics to the third and fourth equations in (2.1.3), there results:

$$\frac{\partial f}{\partial t} = -\frac{\lambda_2 c f}{1 + \nu_2 f}, \tag{2.1.7}$$

where $\lambda_2 = k_4$ and $\nu_2 = k_4/k_3$.[1]

These rate equations then require five initial conditions for v, c, ℓ, r, f. Although the initial condition for r, the number of receptors per endothelial cell, is not known precisely, it is known to be of the order of magnitude $10^5 \pm 10^3$.

The rate equations for fibronectin and protease are not complete as they stand. Endothelial cells are known to produce fibronectin. This production of fibronectin is modeled through a logistic growth term $\beta f(f_M - f)\eta$. Therefore, in the discussion below we replace equation (2.1.7) by

$$\frac{\partial f}{\partial t} = \beta f(f_M - f)\eta - \frac{\lambda_2 c f}{1 + \nu_2 f} \tag{2.1.8}$$

where $\beta > 0$ and f_M is the density of fibronectin in the normal capillary.

Additionally, it is known that protease and fibronectin will decay as a function of a variety of mechanisms that include proteolytic degradation (step 3 in (2.1.6)), and endocytosis by surrounding cells.

In particular, this means that the fourth of equations (2.1.6) should have the form

$$\frac{\partial c}{\partial t} = k_2 \ell - \mu c$$

where μ is a decay constant. For the remainder of this paper we shall take $\mu = 0$ as a "worst case" scenario. This not only simplifies the analytical discussion to follow somewhat, but it also does not significantly affect the numerical computations

[1] The units of k_4 are in reciprocal hours and of the k_3 are reciprocal hours per μM ($1\ \mu\text{M} =$ one micro mole per liter). In terms of the biological literature values for protease decay of fibronectin, K_{cat}, K_m, our constants may be expressed as $\lambda_2 = K_{cat}/K_m$ while $\nu_2 = 1/K_m$. We shall adopt this notation later. That is, whenever we have a (λ, ν) pair which arises from Michealis-Menten kinetics, we shall let $K_m = 1/\nu$ and $K_{cat} = \lambda/\nu$.

which follow that discussion. Indeed, it is clear that μ should have a stabilizing influence on solutions of the systems. We illustrate this numerically. However, it is not easy to find good values for μ. Although some values are known for certain proteases, none of them are for in vivo decay. [2]

We may take $\ell(x, 0) = 0$ as there is no intermediate present initially. Initially there is also very little proteolytic enzyme present so $c(x, 0) \approx 0$.[3]

We can introduce growth factor into the system by prescribing $v(x, 0)$. The major difficulty is in determining $r(x, 0)$, the number of receptors per endothelial cell.

For this reason, as well to simplify the numerical computations and put the problem in as non-dimensionalized a form as is possible, we shall consider the Michealis-Menten approach to (2.1.6). We then try to replace $r(x, t)$ by $\eta(x, t)$. (One can at least hope to be able to count individual endothelial cells in microscopic sections.) Also, endothelial cell motion takes place on a much slower time scale than that of (2.1.6).

Before doing this, notice that if we add the first two (2.1.6) and integrate over time, we obtain the conservation law $r(x, t) + \ell(x, t) = r(x, 0)$. The basic idea underlying the Michealis-Menten hypothesis is to set the right hand side of the first or second equation in (2.1.6) to zero (by assuming that $\epsilon(x) \equiv 1/(k_1 r(x, 0)) = 0$), solve the resulting equation for ℓ and substitute this back into $r(x, t) + \ell(x, t) = r(x, 0)$ to obtain

$$\begin{aligned} r(x, t) &= \frac{r(x, 0)}{1 + \nu_1 v(x, t)} \\ \ell(x, t) &= \frac{\nu_1 r(x, 0) v(x, t)}{1 + \nu_1 v(x, t)} \end{aligned} \tag{2.1.9}$$

where we have set $\nu_1 = k_1/(k_2 + k_{-1})$. However, the first of equations (2.1.9) cannot be correct as it stands at $t = 0$ unless the initial concentration of angiogenic factor is zero. Of course, as pointed out in Murray, [34], Chapter 5, this difficulty arises because the assumption that $\epsilon = 0$ is not consistent with the number of initial conditions needed for the system (2.1.6). In other words, we are dealing with a singular perturbation problem here. The equations (2.1.9) are only valid as part of the so called "outer solution". The outer solution is considered to be valid only for times $t \gg \epsilon$ and must be matched with the so called "inner solution". Murray does this in [34], p. 119.

[2] It should be remarked that in the work we have under way, where we consider the actual penetration of the capillary sprout into the ECM, this term will play a critical role. The reason for this is that in the ECM there is EC cell proliferation and death. This means that the EC cell movement equation must include a source term of the form $N[(1 - N) + G(c)c_t - \sigma]$ where $N(x, y, t)$ resp. $(N(x, y, z, t))$ is the two (resp. three) dimensional EC cell density and $G(c)$ is a biphasic EC mitosis rate term which decays to zero as $c \to +\infty$. The inclusion of the term μc in the enzyme rate law prevents $c \to +\infty$. Further discussion of this here would take us beyond the scope of the present paper.

[3] This background protease cannot be neglected in any models that include $\mu > 0$. We shall deal with this issue in a forthcoming paper.

Murray refers to the outer solution as the "pseudo steady state". He also uses a singular perturbation argument to give a set of circumstances under which (2.1.9) may be justified. These conditions are met here for reaction mechanisms such as (2.1.6) when $k_1 r(x,0)$ is very large. This last condition will hold, not only because k_1 itself is generally large since the forward receptor-ligand reaction is known to proceed very rapidly, but also because $r(x,0)$, the density of receptors on the endothelial cells, is generally much larger than $\eta(x,0)$.

Therefore, on the time scales involved, if we employ the pseudo steady state by using the first of (2.1.9), we obtain for $t \gg \epsilon = \max(1/k_1 r(x,0))$

$$\begin{aligned} \frac{\partial v}{\partial t} &= \frac{-\hat{k}_1 v r(x,0)}{1+\nu_1 v} \\ \frac{\partial c}{\partial t} &= \frac{\hat{k}_1 v r(x,0)}{1+\nu_1 v}. \end{aligned} \tag{2.1.10}$$

where we have set $\hat{k}_1 = \nu_1 k_1$. From now on, $t >> \epsilon$. (Notice that when $k_{-1=0}$, $\hat{k}_1 = k_1$.)

As remarked above, We would like to replace $r(x,0)$ by $\eta(x,t)$ in (2.1.10). To justify this we argue as follows:

The first of (2.1.10) tells us that that the rate $v_t < 0$. This means v approaches some limiting function, $v_\infty(x)$ as $t \to +\infty$. Then, solutions of the first equation behave like solutions of $v_t \approx -s(x)v$ where $s(x) = \hat{k}_1 r(x,0)/(1+\nu_1 v_\infty(x))$. This tells us that $v \to 0^+$ as $t \to +\infty$ exponentially fast (like $\exp(-\hat{k}_1 r(x,0)t)$) at those points where $r(x,0) > 0$. This means we have $r(x,t) \approx r(x,0)$ on the time scale for which the pseudo steady state is valid. (This follows since $0 \le r(x,0) - r(x,t) = \ell(x,t) \le \nu_1 r(x,0) v(x,t) \to 0$.)

With this understanding the equations (2.1.10) can be replaced by

$$\begin{aligned} \frac{\partial v}{\partial t} &= \frac{-\hat{k}_1 v r(x,t)}{1+\nu_1 v} \\ \frac{\partial c}{\partial t} &= \frac{\hat{k}_1 v r(x,t)}{1+\nu_1 v}. \end{aligned} \tag{2.1.11}$$

In passing from (2.1.10) to (2.1.11), we are making an absolute error in the time derivatives of no more than $\hat{k}_1(r(x,0)-r(x,t))v/(1+\nu_1 v) \le \hat{k}_1 \ell(x,t) v/(1+\nu_1 v)$ which in turn is smaller than $\hat{k}_1 r(x,0) v^2/(1+\nu_1 v)^2$. This upper bound approaches zero faster than $\exp(-2\hat{k}_1 r(x,0)t)$ which is much faster than the approach of v to zero.[4]

[4] More precisely, if (v,c) is a solution of (2.1.10) and (v',c') is a solution of (2.1.11) with the same initial conditions and if we set $w = v - v'$, then

$$w_t = -\frac{\hat{k}_1 \ell v}{1+\nu_1 v} - \frac{\hat{k}_1 r w}{(1+\nu_1 v)(1+\nu_1 v')}.$$

Therefore the difference between v and v' (as well as between c and c') decays to zero even faster than $\exp(-\hat{k}_1 r(x,0)t)$ due to the contribution of the first term on the right of the above equation.

To complete our discussion, we further exploit the relationship between cell density and receptor density. In general, the the number of receptors per cell, $r(x,t)/\eta(x,t)$, which we denote by $\delta(x,t)$, is nearly constant although it may vary somewhat with η, for example, if the cells are closely packed or after initiation of cell proliferation and movement. We need to do this because, while we have good estimates of the number of receptors per cell, it is the number of cells per unit length which we can, in principle, directly observe in sections of tissue under the microscope. In turn, this linear cell density must be converted to a volumetric density expressed in micro moles per liter.[5] To find the volumetric density, we imagine the cells to be small rectangular parallelepipeds.

Since capillaries have a diameter of about 6–8 microns and red blood cells have a diameter of 4–5 microns, we can estimate the the thickness of an endothelial cell to be about 1 micron with a width of about $7\pi/2 \approx 10$ microns. (The thickness of the basement membrane itself is much smaller than that of an EC and is neglected.) It is known that there are about 10–100 EC per millimeter so that their length can be taken to be between 10 and 100 microns. This means that the volumetric density of endothelial cells is roughly of the order of 10^{12} cells per liter. (The dimensions of an endothelial cell are taken from [36].) The number of receptors per cell is of the order of 10^5 [7,59]. Therefore, for the purposes of this model the receptor density is viewed as a concentration $\delta\eta_0 \approx 10^{17}$ per liter or 10^{-6}M or one μM.

Therefore, we can write

$$\begin{aligned} \frac{\partial v}{\partial t} &= \frac{-\lambda_1 v\eta(x,t)}{1+\nu_1 v} \\ \frac{\partial c}{\partial t} &= \frac{\lambda_1 v\eta(x,t)}{1+\nu_1 v} \end{aligned} \tag{2.1.12}$$

where now $\lambda_1 = \hat{k}_1\delta$ and we understand that $t \gg 1/\hat{k}_1\delta$.

Remark 1. In principle, one should consider adding stabilizing terms such as $D_v v_{xx}$, $D_c c_{xx}$, $D_f f_{xx}$ to equations (2.1.12) and (2.1.7). However this is not realistic for the biological situation we are considering here. Fibronectin is not expected to diffuse much through the protein matrix along the ablumenal capillary surface.

Also, along this surface, the removal of v and the increase in c are likely to be on a much faster exponential time scale than their diffusion along this surface, so it seems reasonable to neglect diffusion rates by comparison with reaction rates, especially as these proteins bind to many components of the ECM.

In particular, growth factor is converted almost immediately into activated receptor complex upon arrival at the capillary wall via the above reactions so that very little if any of it is left to diffuse along the capillary lumen.[6]

[5] The issue of units is quite important. In order to relate the constants k_i to literature values where the terminology, K_{cat}, K_m is used, the concentrations of the chemical species in (2.1.11) must be expressed in volumetric units, say in micro moles per liter.

[6] This assumes that the rate of supply of the growth factor at the wall is insufficient to generate quantities of growth factor to saturate all or nearly all the available EC receptors.

The diffusion of growth factors cannot be neglected in the ECM in the full model we are developing in [30] since it is known that these proteins can diffuse several cell diameters before they are degraded or depleted.

Mathematically, diffusion provides the transport mechanism in the model for growth factor to move from the tumor to the capillary.

The situation here is also in marked contrast to that in the case of wound healing. There, growth factors are released by damaged cells. Plasma can also generate growth factors. Thus growth factor diffusion in the plasma must be considered at the outset.

We next turn to the issue of cell movement.

2.2. Reinforced random walk

Before beginning our discussion of reinforced random walk, we want to emphasize the role of time scales once more. Endothelial cells move at a much slower rate than the rate at which the kinetic equations above come to pseudo steady state. That is, time scales for the former movements are of the order L^2/D whereas the time scales for the latter are $\epsilon = 1/(\hat{k}_1\delta\eta_0) = K_m/(K_{cat}\delta\eta_0)$. Typically, $L^2/D \approx 100$ days[7] while $\epsilon \approx 50$ seconds (using the observation that $\delta\eta_0 \approx 1\ \mu$M and data from[28]).

Therefore, in the discussion below, we shall assume that the biochemistry of the motion, i.e., the kinetic equations (2.1.6) are already in pseudo steady state, i.e. that equations (2.1.12) are in force at time $t = 0$, the dynamics having been initiated at some time $-\bar{t} < 0$ *before the endothelial cells have begun to move.* From now on, time is positive.

In order to understand the idea behind the notion of reinforced random walks, we consider the parent capillary wall to be a one dimensional lattice with endothelial cells (assumed to be a mono-layer of equal size and shape) equally spaced and in non-overlapping contact located at reference points nh along the x-axis.

Let $\hat{\tau}_n^{\pm}(W)$, depending upon the control substances W, be the transition probability rate per unit time for a one-step move of an endothelial cell at site n to site $n+1$ or $n-1$ respectively. Let $\eta_n(t)$ be the probability density distribution of the endothelial cells at position nh at time t. Then the time rate of change of $\eta_n(t)$ is governed by the master equation:

$$\frac{\partial\eta_n(t)}{\partial t} = \hat{\tau}_{n-1}^{+}(W)\eta_{n-1} + \hat{\tau}_{n+1}^{-}(W)\eta_{n+1} - (\hat{\tau}_n^{+}(W) + \hat{\tau}_n^{-}(W))\eta_n. \qquad (2.2.1)$$

That is, η_n will be augmented by cells moving from the positions $(n \pm 1)h$ to nh and diminished by cells moving from nh to either $(n+1)h$ or $(n-1)h$. The quantity $(\hat{\tau}_n^{+}(W) + \hat{\tau}_n^{-}(W))^{-1}$ is the mean waiting time at site n.

It is convenient to think of this conditional probability density as the density of endothelial cells. The point of view adopted here is the same as in quantum mechanics where an electron can be thought of as a probability density or else as an " electron cloud of negative charge."

[7] EC movement values here are of the order $10^{-11}\text{cm}^2/\text{sec}$ [52].

The transition probability rates $\hat{\tau}_n^{\pm}(\cdot)$ depend on control substances which we have denoted by W and are defined on the lattice at $\frac{1}{2}$-step size. The control substances W are very general and can include all products which are generated in response to the growth factors described above i.e., FGF, VEGF, TGFα, TGFβ, etc. However, in this paper, we emphasize the important role of fibronectin, an ECM component, and proteolytic enzyme which degrades the ECM and ruptures the basement membrane. The control substance W is represented as the vector of components.

$$W = (...W_{-n-\frac{1}{2}}, W_{-n}, W_{-n+\frac{1}{2}}, ...) \tag{2.2.2}$$

where $W_n = W_n(f, c)$ depends on the concentration of proteolytic enzyme (c) and the fibronectin (f) at that lattice point.

While the basic model (2.2.1) can be exploited [41] to describe many aspects of organism dynamics it gives no restriction on the transition rates at a site and there is no correlation between transition rates to right or left.

Suppose, as suggested in [41], that the decision of "when to move" is independent of the decision of "where to move". Then the mean waiting time of the process is constant across the lattice. Hence the transitions $\hat{\tau}_n^{\pm}$ must be suitably scaled and normalized so that

$$\hat{\tau}_n^{+}(W) + \hat{\tau}_n^{-}(W) = 2\lambda, \tag{2.2.3}$$

where λ is a scaling parameter. Let the transition rates depend on W only at the nearest neighbors, $W_{n\pm\frac{1}{2}}$. In order to achieve (2.2.3) define the new jump process τ by

$$\hat{\tau}_n^{\pm}(W) = 2\lambda \frac{\tau(W_{n\pm\frac{1}{2}})}{\tau(W_{n+\frac{1}{2}}) + \tau(W_{n-\frac{1}{2}})} \equiv 2\lambda N^{\pm}(W). \tag{2.2.4}$$

The master equation now reads

$$\begin{aligned} \frac{1}{2\lambda}\frac{\partial \eta_n}{\partial t} &= N^{+}(W_{n-\frac{1}{2}}, W_{n-\frac{3}{2}})\eta_{n-1} + N^{-}(W_{n+\frac{1}{2}}, W_{n+\frac{3}{2}})\eta_{n+1} \\ &\quad -[N^{+}(W_{n+\frac{1}{2}}, W_{n-\frac{1}{2}}) + N^{-}(W_{n-\frac{1}{2}}, W_{n+\frac{1}{2}})]\eta_n. \end{aligned} \tag{2.2.5}$$

We now proceed to the continuous limit by letting $h \to 0$ and $\lambda \to +\infty$ in such a way that

$$D = \frac{1}{2}\lim_{h\to 0, \lambda\to+\infty} \lambda h^2. \tag{2.2.6}$$

(See [31,41] for details) to obtain the primary equation, which we shall refer to as the continuous limit of master equation (CLME):

$$\frac{\partial \eta}{\partial t} = D\frac{\partial}{\partial x}\left(\eta \frac{\partial}{\partial x}\left(\ln \frac{\eta}{\tau}\right)\right) \tag{2.2.7}$$

where $\eta(x,t)$ now denotes endothelial cell density and $\tau = \tau(w) = \tau(w(f,c))$.[8]

We also have the dynamical equation for fibronectin, (2.1.8) and initial condition:

$$\begin{aligned} \frac{\partial f}{\partial t} &= \beta f\,(f_M - f)\,\eta - \tfrac{\lambda_2 c f}{1+\nu_2 f}, \\ f(x,0) &= f_M(x) > 0 \end{aligned} \tag{2.2.9}$$

where we have set $k_3 = \lambda_2$.

We also have in addition to (2.2.7), (2.2.9), the pair of equations (2.1.12) as well as the initial conditions

$$\begin{aligned} v(x,0) &= v_0(x) > 0, \\ c(x,0) &= c_0(x) \geq 0. \end{aligned} \tag{2.2.10}$$

The system is closed by assuming no-flux boundary conditions at $x = 0, \ell$, i.e.

$$\eta \frac{\partial}{\partial x}\left(\ln \frac{\eta}{\tau}\right) = 0 \quad \text{at} \quad x = 0, \ell. \tag{2.2.11}$$

To complete the model we suppose the transition probability rate function τ to be factored as

$$\tau\,(w\,(f,c)) = \tau_1\,(c)\,\tau_2\,(f\,) \tag{2.2.12}$$

These factors are chosen in order to provide a measure of how responsive endothelial cells are to protease and to fibronectin. It is known that proteases stimulate the movement of endothelial cells, [20, 33, 48, 51]. In [20] for example, it was shown that protease inhibitors can inhibit EC migration.

It is also reasonable to suppose that $\tau_2(f)$ is a decreasing function of f. That is, endothelial cells are attracted to sites of low fibronectin or collagen density [8, 14, 21, 35, 56]. For example, in [35], the authors conclude that the data from their experiments.

"support the hypothesis that fibronectin promotes angiogenesis and suggest that developing micro-vessels elongate in response to fibronectin as a result of an adhesion-dependent migratory recruitment of endothelial cells that does not require increased cell proliferation".

(The choice we make below for τ is somewhat analogous to the assumption of a linear relation between stress and strain that is is made in the classical theory of Newtonian fluid flow. This is an ad hoc postulate, not derivable on the basis of

[8] Equation (2.2.7) can be written in the more standard form

$$\eta_t = D\eta_{xx} - D\left(\eta \frac{\tau_c c_x + \tau_f f_x}{\tau(c,f)}\right)_x = D\eta_{xx} - D(\eta(\ln \tau)_x)_x \tag{2.2.8}$$

which may be a form more familiar to some readers. However, if one thinks of (2.2.7) as a diffusion process for reinforced random walk, then the long time tendency for such a process will be to drive η in such a way as to bring the ratio η/τ to unity. In other words, the "walker density equation" asserts that the walker will move in such a way as to have a large probability density where the probability transition rate is large and a small probability density where it is small.

statistical mechanics or any other "first principle." But as an assumption about the nature of Newtonian fluids, its validity is unquestioned. Our view here is that the choice we make for τ here will have similar descriptive and predictive success.)

We suppose therefore that the τ_i obey power laws. This is admittedly a first step in modeling τ. In particular, we write them as

$$\begin{aligned} \tau_1(c) &= c^{\tilde{\gamma_1}/D} \\ \tau_2(f) &= f^{-\tilde{\gamma_2}/D} \end{aligned} \tag{2.2.13}$$

where $\tilde{\gamma_1}, \tilde{\gamma_2}$ are positive (unknown at the present time) constants. These lead to a chemotactic sensitivity

$$\chi_c \equiv \frac{\tau_1'(c)}{\tau_1(c)} = \frac{\tilde{\gamma_1}}{Dc} \tag{2.2.14}$$

and a haptotactic sensitivity

$$\chi_f \equiv \frac{\tau_2'(f)}{\tau_2(f)} = \frac{-\tilde{\gamma_2}}{Df}. \tag{2.2.15}$$

respectively. We shall say that the sensitivity factors (2.2.15), (2.2.14) are "power law sensitivity factors". The choice of the transition probability τ adopted here is to provide a measure of how responsive the EC are to various growth factors. In the case of tumor growth this would be for example due to the EC's cellular responses to one or more of the tumor angiogenesis factors (TAF). The model is in this regard very flexible and other choices of τ can be adopted, having other degrees of sensitivity depending on the particular angiogenic process to be modeled. For example in [41] it is supposed that a signal is transduced via a receptor R which binds with the signal w and that the response is proportional to the fraction of receptors occupied. The binding reaction can be written as

$$R + w \underset{k_{-1}}{\overset{k_1}{\rightleftarrows}} [Rw] \tag{2.2.16}$$

where $[Rw]$ denotes the receptor–ligand complex. If binding comes rapidly to equilibrium on the time scale of the evolution of η and w, then for the local sensing, in [41], the authors choose a transition probability

$$\tau(w) = \frac{\beta w}{\gamma + w}, \tag{2.2.17}$$

where β is a constant that incorporates the total number of receptors and $\gamma \equiv k_{-1}/\hat{k}_1$.

In their work on modeling capillary endothelial cell-extracellular matrix interactions in wound healing, the authors in [38] used a haptotactic transition probability.

$$\tau(m) = \quad \exp \quad C(k+m)^{-1} \tag{2.2.18}$$

where C and k are constants and m is the fibrillar ECM density.

While the transition probabilities in (2.2.13) are a possible first step in modeling the response of the endothelial cells to enzyme and fibronectin densities they

show singular behavior for small and large values of c, f respectively. Therefore in Section 3 of this paper we shall consider a mollified form of $\tau(c, f)$ given by

$$\begin{aligned}\tau(c, f) &= \tau_1(c)\,\tau_2(f)\\ &= \left(\frac{\alpha_1 + c}{\alpha_2 + c}\right)^{\gamma_1}\left(\frac{\beta_1 + f}{\beta_2 + f}\right)^{\gamma_2}\end{aligned} \tag{2.2.19}$$

where $\alpha_i, \beta_i, \gamma_i$ are positive constants. We refer to the sensitivity factors coming from (2.2.19) as "saturable sensitivity factors". ("Mollified" means that the function is bounded away from zero and infinity.) The assumption here is that $0 < \alpha_1 \ll \alpha_2$ to model $c^{m/D}$ for $m = \tilde{\gamma_1} = D\gamma_1 > 0$ and $0 < \beta_2 \ll \beta_1$ to model $f^{m/D}$ where $m = -\tilde{\gamma_2} = -D\gamma_2 < 0$.

These saturable sensitivity factors then take the form:

$$\chi_c = \gamma_1 \frac{\alpha_2 - \alpha_1}{(\alpha_1 + c)(\alpha_2 + c)}, \tag{2.2.20}$$

$$\chi_f = \gamma_2 \frac{\beta_2 - \beta_1}{(\beta_1 + f)(\beta_2 + f)}. \tag{2.2.21}$$

Suppose that we have a capillary segment of length ℓ. If we apply the scaling $x' = x/\ell$ then we can work on the unit interval $[0, 1]$ provided that we remember that D is to be replaced by D/ℓ^2 in our calculations. In summary, then, we will consider the following initial-boundary value problem in the sequel. The goal is to solve the problem numerically and then to interpret the results biologically.

$$\begin{aligned}\frac{\partial \eta}{\partial t} &= D\frac{\partial}{\partial x}\left(\eta\frac{\partial}{\partial x}\left(ln\frac{\eta}{\tau}\right)\right),\\ \frac{\partial v}{\partial t} &= \frac{-\lambda_1 v\eta}{1 + \nu_1 v},\\ \frac{\partial c}{\partial t} &= \frac{\lambda_1 v\eta}{1 + \nu_1 v},\\ \frac{\partial f}{\partial t} &= \beta f\,(f_M - f)\,\eta - \frac{\lambda_2 cf}{1 + \nu_2 f},\\ \eta\frac{\partial}{\partial x}\left(ln\frac{\eta}{\tau}\right) &= 0, \quad x = 0, 1.\end{aligned} \tag{2.2.22}$$

together with the initial conditions

$$\begin{aligned}\eta(x, 0) &= \eta_0(x) \geq 0,\\ v(x, 0) &= v_0(x) \geq 0,\\ c(x, 0) &= c_0(x) \geq 0,\\ f(x, 0) &= f_M(x) \geq 0.\end{aligned} \tag{2.2.23}$$

For example, in the most important case, all of the initial conditions in (2.2.23) are constant except possibly v_0. (Indeed, in our simulations, we will normalize our

equations so that $f_M = 1$, $\eta_0 = 1$[9] and assume that no enzyme is present initially so $c_0(x) = 0$.) If there is no angiogenic factor initially present, then $v_0 = 0$.

3. Numerical experiments

In this section we present some numerical computations for the system (2.2.22) together with initial conditions

$$\begin{aligned} \eta(x,0) &= \eta_0, \\ v(x,0) &= v_0\kappa_m(1-\cos(2\pi x))^m > 0, \\ c(x,0) &= c_0 = 0. \\ f(x,0) &= f_M. \end{aligned} \tag{3.1}$$

where v_0, κ_m, m are positive constants. The constant κ_m is chosen so that $\int_0^1 v(x,0)\,dx = v_0$. We use the choice for τ given by (2.2.19). The constant m is to be thought of as a measure of how "concentrated" or localized the angiogenic factor is. That is, the sequence of functions $\{F_m(x) \equiv \kappa_m[1-\cos(2\pi x)]^m\}_1^\infty$ forms a δ sequence.[10]

This is the type of problem one might consider if a small amount of angiogenic growth factor were supplied to the rest state suddenly, or over a time scale that is very small in comparison to that for (2.2.22). (That is, as unit impulse data.)

We also discuss the related system of forced equations:

$$\begin{aligned} \frac{\partial \eta}{\partial t} &= D\frac{\partial}{\partial x}\left(\eta\frac{\partial}{\partial x}\left(ln\frac{\eta}{\tau}\right)\right), \\ \frac{\partial v}{\partial t} &= \frac{-\lambda_1 v\eta}{1+\nu_1 v} + v_r(x,t), \\ \frac{\partial c}{\partial t} &= \frac{\lambda_1 v\eta}{1+\nu_1 v}, \\ \frac{\partial f}{\partial t} &= \beta f(f_M - f)\eta - \frac{\lambda_2 cf}{1+\nu_2 f}, \end{aligned} \tag{3.2}$$

together with

$$\begin{aligned} \eta(x,0) &= \eta_0, \\ v(x,0) &= v_0 = 0, \\ c(x,0) &= c_0 = 0. \\ f(x,0) &= f_M. \end{aligned} \tag{3.3}$$

and angiogenic factor $v_r(x,t)$ given by

$$v_r(x,t) = v_0\kappa_m[1-\cos(2\pi x)]^m e^{-\theta t}. \tag{3.4}$$

[9] When we normalize η by replacing η by η/η_0 then $\lambda_1\eta_0 = \hat{k}_1\delta\eta_0 \approx K_{cat}/K_m$ since $\delta\eta_0 \approx 1\mu M$.

[10] We have $\lim_{m\to+\infty} F_m(x) = \delta(x-\frac{1}{2})$ the δ function concentrated at $x = 1/2$, in the sense of distributions.

Table 1. Parameters and biological constants

$\eta(x,t)$ (Endothelial cell movement)	$D = 3.6 \times 10^{-5}$	$\alpha_1 = 0.001$	$\alpha_2 = 1.0$	$\gamma_1 = 1.2$
η (EC movement continued)	$\beta_1 = 1.0$	$\beta_2 = 0.001$	$\gamma_2 = 1.2$	
v (Angiogenic factor kinetics)	$\lambda_1 = 73.0$	$\nu_1 = 0.007$	$m = 100$	$v_0 = 15$
c (Proteolytic enzyme kinetics)	$\lambda_1 = 73.0$	$\nu_1 = 0.007$		
f (Fibronectin rate law)	$\beta = 0.222$	$\lambda_2 = 19.0$	$\nu_2 = 1.28$	

Now $\int_0^1 v_r(x,t)\,dx = v_0 e^{-\theta t}$ where $m, \theta > 0$. The constant v_0 is now a measure of the average rate of supply of growth factor.

This is the type of problem in which one might envisage a rate of supply of growth factor from a tumor somewhat removed from the capillary but which has arrived at the capillary wall via diffusion. We might expect that for a real tumor, $\theta > 0$. That is, the production of TAF cannot be sustained for an avascular tumor. The worst case occurs when $\theta = 0$.

A word about the choice of constants: Good biological constants for events occuring in vivo are notoriously hard to come by. This is further complicated by the fact that under the general rubric "fibronectin", for example, are a whole host of ECM proteins including the very familiar collagens. Also, there are many different growth factors. Further complicating these issues is the fact that much of the data we have is "in vitro" data. In the living organism, the situation may be quite different. For example, it is known that some growth factors stimulate proliferation or cell movement in vivo but inhibit growth in vitro or vice versa, [29].

Never-the-less, we have to start somewhere. Therefore, we have taken values from the literature that are representative of the mechanisms proposed here.

All volumetric units are in micro molarity, the time scale is in hours, the length scale is in microns. We re-scale by taking $\eta_0 = 1$. Since, $\delta\eta_0 = 1\mu$M, we can take the constants λ_i as K^i_{cat}/K^i_m and $\nu_i = 1/K^i_m$.

We used the following values for our constants in our first set of experiments:

The choice of these constants was dictated by the following considerations:

The sensitivity parameters, α_i, β_i, γ_i were chosen for illustrative purposes only. They must be determined experimentally and this has yet to be done.

Since we know that the average capillary diameter is about $6-8\mu$m or $0.006-0.008$ mm in diameter, the scale we have chosen is such that $x = 1$ corresponds to 50 microns. Experimentation with the power m indicates that when $m = 100$ the opening in the simulated nascent capillary will be roughly in range $6-8\mu$m.

The cell movement constants above are of the order of magnitude found in [52] when expressed in units of mm^2/hr. For example, 10^{-10}cm^2/sec $= 3.6\times10^{-7}$cm^2/$h = 3.6 \times 10^{-5}$mm$^2/h$.

The values taken from [28] for the VEGF receptor yield $\lambda_1 = K_{cat}/K_m \approx 162 \times 60/130 \approx 73$ per μM per hour and $K_m \approx 130\,\mu M$. This gives a corresponding value for $\nu_1 \approx 0.007\mu M^{-1}$.

For the constants in the "fibronectin" production equation, we have taken values for λ_2, ν_2 from [16]. We took $K_{cat} = 16$ per hour and $K_m = 0.83\ \mu$M for the hydrolysis of type I collagen (rat tendon) human fibroblast collagenase.

The constant β is estimated as follows. We know that in $T = 18$ hours, f_M moles of fibronectin will be generated by η_0 endothelial cells, [60, 39]. In the absence of protease, we have $f_t = \beta_1 f(f_M - f)\eta_0$ so that approximately, we can write $f_M/T \approx \beta_1 \eta_0 f_M^2 x(1-x)$ where $x = f/f_M$. The maximum value of $x(1-x)$ on [0, 1] is 0.25. This gives a minimum possible value $\beta_1 \approx 4/(T f_M \eta_0)$. Renormalizing the equation $f_t = \beta_1 f(f_M - f)\eta - c\lambda_2 f/(1 + \nu_2 f)$ so that $\eta_0 = 1$ and $f_M = 1$ we have $\beta = \beta_1 \eta_0 f_M = 4/T \approx 0.22h^{-1}$. This renormalization will involve replacing ν_2 by $\nu_2 f_M$.

We see that we have at our disposal the dosage constant v_0, the chemotactic and haptotactic sensitivities, α_i, β_i, γ_i and a constant m which is a measure of the support of the growth factor, i.e., the larger m is, the more "δ-function like" will be the data function.

The above values were used in all of our figures unless otherwise stated in the captions or on the figures themselves.

The Figures 5–9 present the results of numerical experimentation with (2.2.22)-(2.2.23). With $m = 100$ we see that the fibronectin density rapidly decays in the interval $0.44 < x < 0.56$ which has a length of $0.12 \times 5\mu$m or about 6 microns. It is in this interval where the growth factor is most highly concentrated at the outset. The channel width is in the range of a typical capillary diameter.

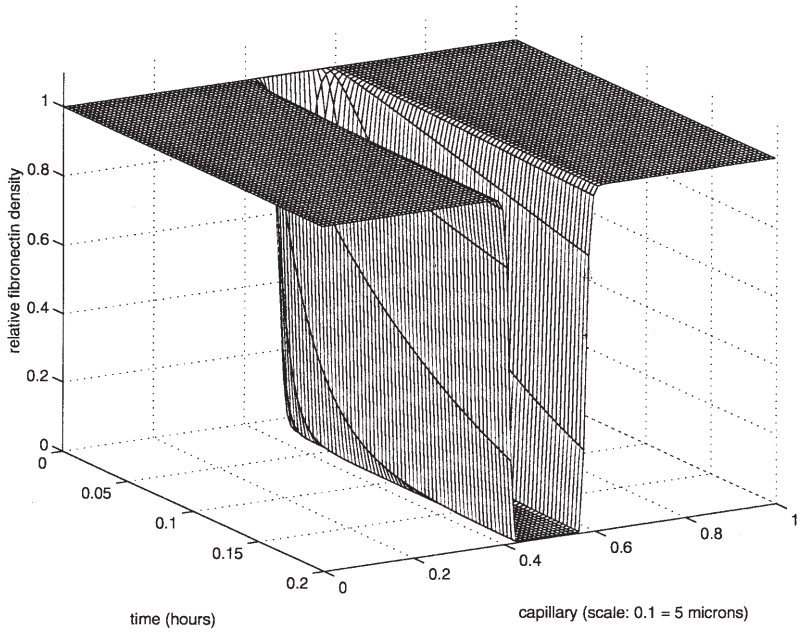

Fig. 5. Time evolution of the onset of angiogenesis for system (2.2.22)–(2.2.23). Time evolution of fibronectin decay. The opening is about 8 μM.

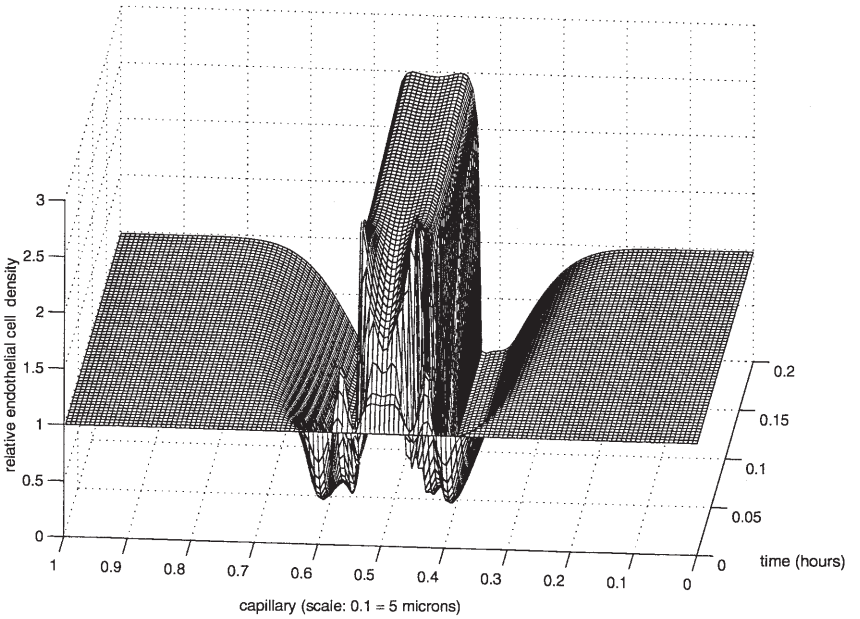

Fig. 6. Time evolution of the onset of angiogenesis for system (2.2.22)–(2.2.23). Time evolution of endothelial cell movement. Notice the bimodality for each time slice. We took $\Delta t = 10^{-4}$, $\Delta x = 2.5 \times 10^{-3}$. The figure fails to correctly capture the events on the time interval $[0, 0.05]$ where the growth factor is changing most rapidly (see Figure 7). The numerical solution will break down in finite time not much beyond 0.2 hours. (Not shown.) Interestingly, as this occurs, the two maxima coalesce into a single peak.

In Figures 6 and 7, the response of the EC to the angiogenic stimulus is shown to form a bimodal structure of aggregation. It is suggestive of a primitive lining to the emerging capillary sprout. This should be compared with Figures 3 and 4 together with the discussion in the Appendix 7, Subsection 7.4.

Figure 8 illustrates the rapid uptake of growth factor by the EC. We notice the rapid decay of growth factor together with the the convergence of the proteolytic enzyme to a steady state as shown in Figure 9.

In Figures 10–12, we have carried out experiments to determine the effects of the localization of $v(x, 0)$ as regulated by the parameter m. In Figure 10, we see that the fibronectin degradation becomes more localized as m increases. Not surprisingly this has the consequence of increased endothelial cell aggregation (Figure 11) while preserving the bimodal structure of the distribution. For comparison we show the superimposed results in Figure 12 for $m = 50$. Figures 13–14 illustrate the evolution of fibronectin and EC concentrations as we change the mean value, v_0, of the initial angiogenic stimulus.

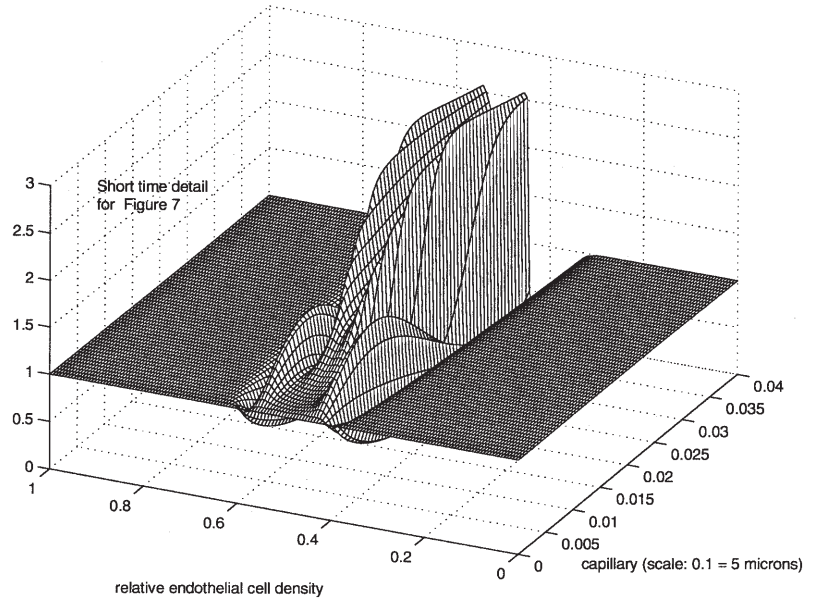

Fig. 7. Time evolution of the onset of angiogenesis for system (2.2.22)–(2.2.23). To better capture the events on the time interval $[0, 0.05]$ where the growth factor is changing most rapidly we took $\Delta t = 10^{-5}$, $\Delta x = 1.25 \times 10^{-3}$. The bimodality of EC distribution is present almost from the outset.

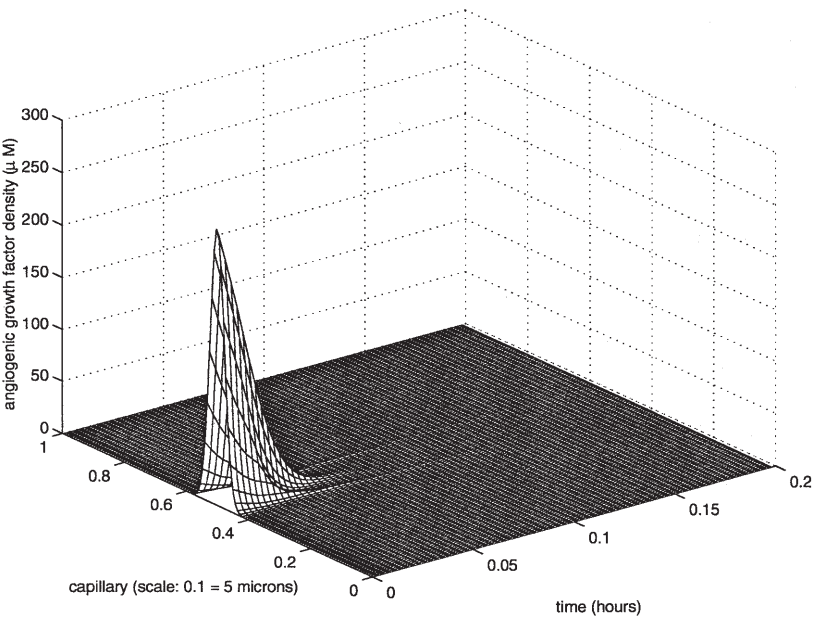

Fig. 8. Time evolution of the onset of angiogenesis for system (2.2.22)–(2.2.23). Time evolution for growth factor decay. Notice that most of the growth factor is gone within 0.025 hours.

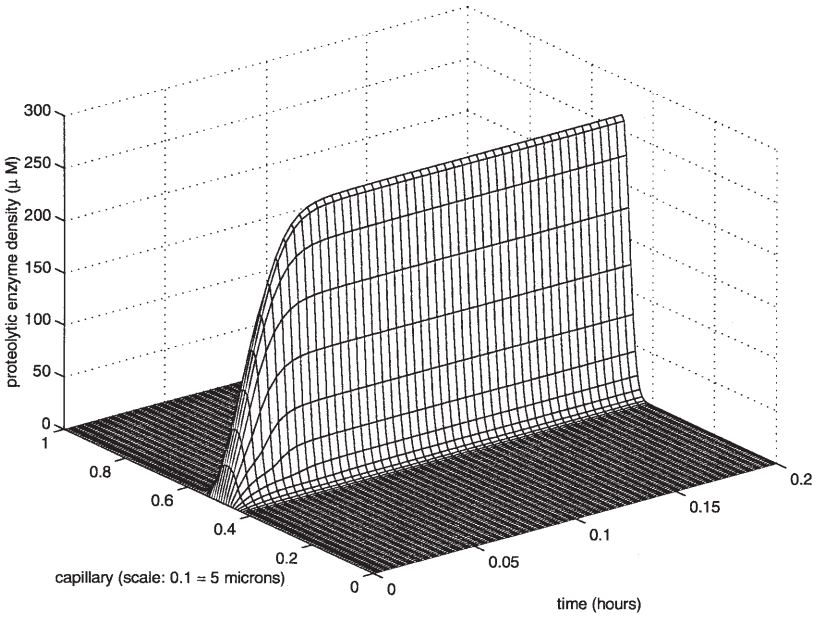

Fig. 9. Time evolution of the onset of angiogenesis for system (2.2.22)–(2.2.23). Time evolution for protease growth. Notice that the concentration of protease has nearly come to a steady state.

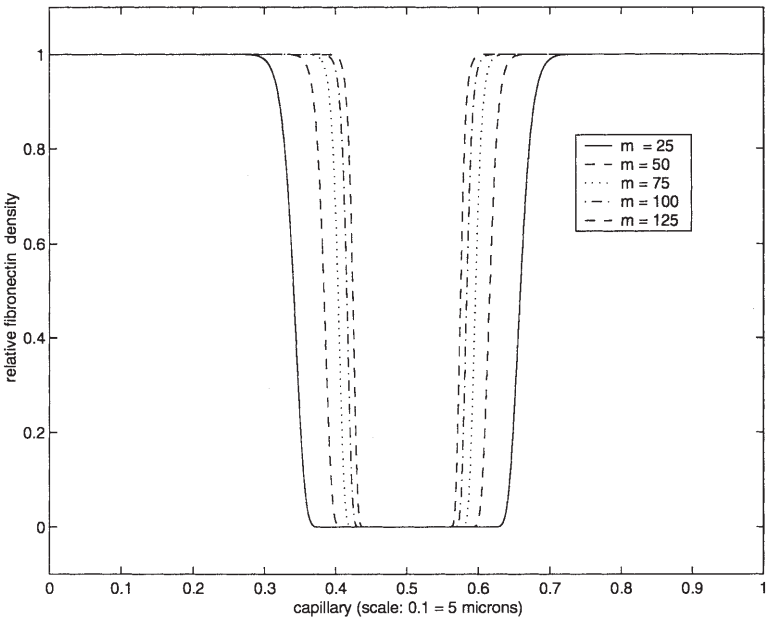

Fig. 10. Dependence of the opening on the initial gradient in $v(x, 0)$ (the parameter m) for (2.2.22)–(2.2.23). Fibronectin densities at $t = 0.2$ hours. As m increases, the gap narrows.

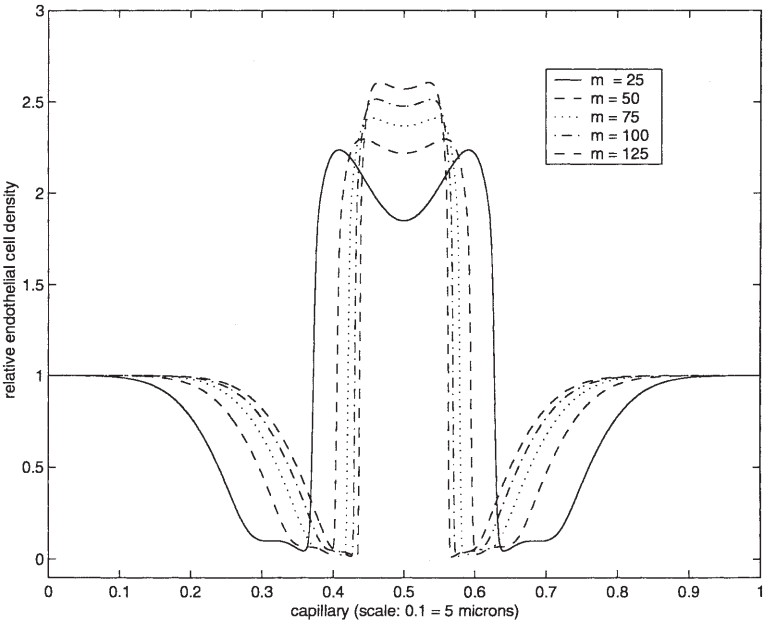

Fig. 11. Dependence of the opening on the initial gradient in $v(x, 0)$ (the parameter m) for (2.2.22)–(2.2.23). Endothelial cell densities at $t = 0.2$ hours. Notice that as m increases, the two maxima coalesce.

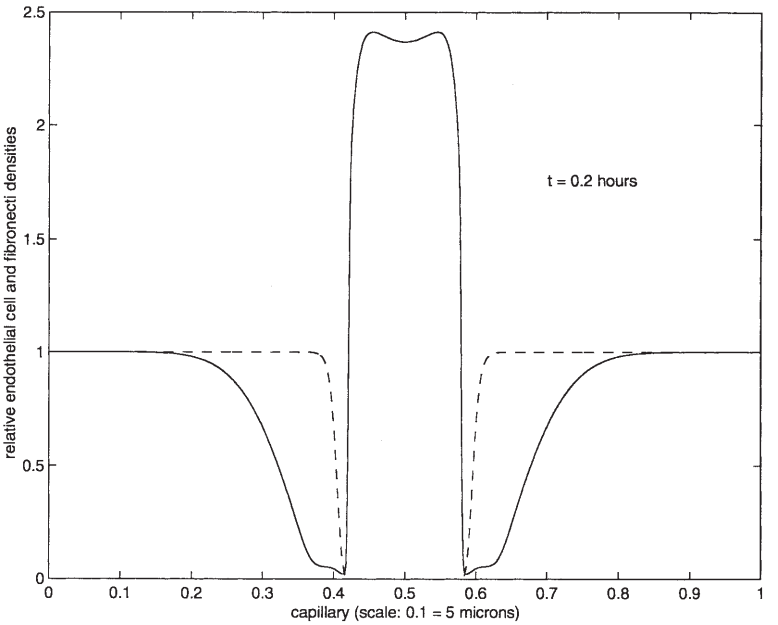

Fig. 12. Dependence of the opening on the initial gradient in $v(x, 0)$ (the parameter m) for (2.2.22)–(2.2.23). Endothelial cell and fibronectin densities for $m = 50$.

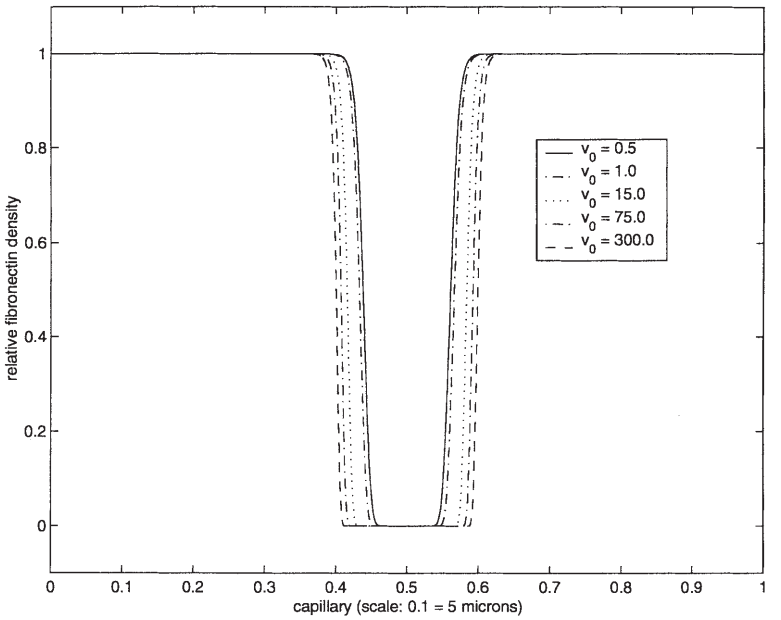

Fig. 13. Dependence of the opening on the initial dosage in $v(x, 0)$ (the parameter v_0) for (2.2.22)–(2.2.23). Fibronectin densities at $t = 0.2$ hours. Notice that as v_0 increases, the size of the opening increases.

4. Note on numerics

Numerical computations with these models can sometimes give misleading information. In our program we used a simple explicit marching procedure. For the standard heat equation, this procedure will be stable if $\delta \equiv D\Delta t/(\Delta x)^2$ is smaller than 0.5. However, for nonlinear problems of the type considered here, this criterion must be modified and the modified criterion checked at each time step. While we did not do this here since it slows the running time, we reran the program at various values of this ratio and decreasing step sizes as a check for consistency.

Furthermore, as in all numerical computations, decreasing step size is not a guarantee of convergence to the true solution as round off error will ultimately defeat this procedure. In the computations we present below, we proceeded along these lines with various δ ratios which satisfied the CFL condition until round off error interfered.

Features of the plots that persisted are presumed to be present in the actual solution while features that depend on the step sizes are assumed to be artifacts of the numerics. A good example of this is illustrated in Figures 6, 7. In Figure 6, for times less than 0.05 hours there appears to be a maximum in $\eta(\cdot, t)$ at $x = 0.5$ which gradually disappears as t increases beyond 0.05. However, when the step size was refined over the shorter interval $[0, 0.05]$, this central maximum disappeared (Figure 7). Thus bimodality occurs from the outset as the theory discussed

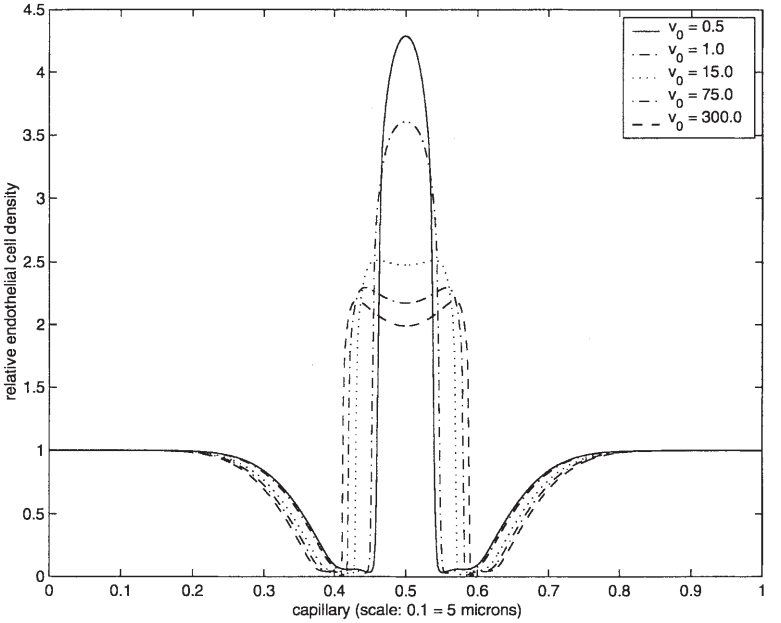

Fig. 14. Dependence of the opening on the initial dosage in $v(x, 0)$ (the parameter v_0) for (2.2.22)–(2.2.23). Endothelial cell densities at $t = 0.2$ hours. Notice that as v_0 increases, the EC distribution passes from unimodal to bimodal.

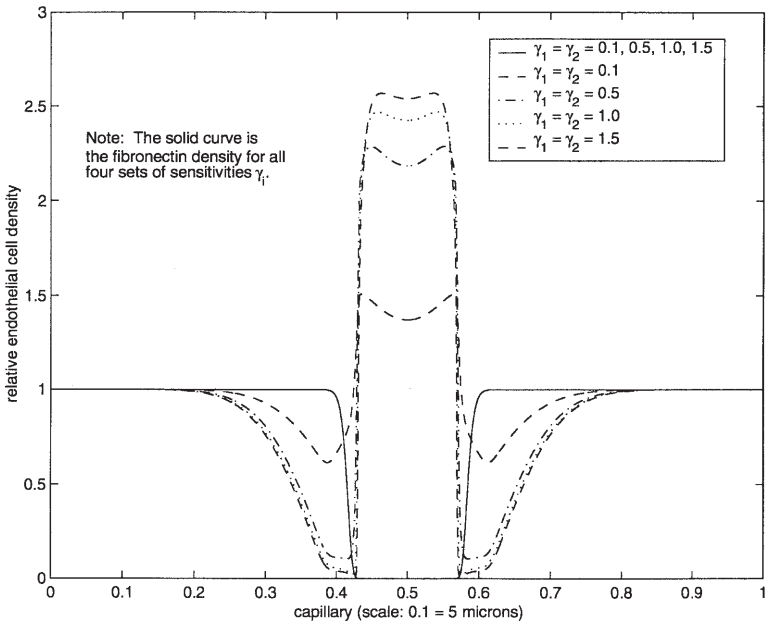

Fig. 15. Dependence of the opening on the sensitivity powers in τ for (2.2.22)–(2.2.23). Here $m = 100$. Notice that as the sensitivities increase, bimodality is decreased.

in the Appendix (Section 7) suggests. See the Appendix, Subsection 7.1. (See also Figures 19–21 and the discussion in the Appendix concerning them.)

The central reason for the difference between Figures 6 and 7 is that in the former figure, the step size in time was too large to capture the effect of the rapidly changing concentration of growth factor on the interval [0, 0.05]. Notice, in Figure 8, that the growth factor decays to practically to zero over this time interval. (For Figure 6 we used $\Delta t = 10^{-4}$ $\Delta x = 2.5 \times 10^{-3}$ as mesh parameters, while Figure 7 we used $\Delta t = 10^{-5}$, $\Delta x = 1.25 \times 10^{-3}$. The latter choice gave a much better resolution of the EC concentration on the time interval [0, 0.05] providing us with 20 times as many grid points as the former choice. Further refinements did not change Figure 7.)

As an additional check on our numerical computations we calculated

$$I(t) \equiv \int_0^1 \eta(x, t)\, dx$$

as

$$I(t) \approx \frac{1}{N} \sum_{i=1}^{N} \eta(i/N, t)$$

which should be constant in time.

5. Summary

In this paper we have set out to describe the essential features of angiogenesis in general and to tumor angiogenesis in particular. This model is based on the cell biologist's observations concerning cell movement. In the case of endothelial cells, it is known that these are more likely to move to places where fibronectin density is low, although not necessarily zero [10], to follow a chemical trail consisting of growth factor and to respond to growth factor by moving into new space created by an enzyme they produce that in turn destroys fibronectin as well as other ECM components.

However complicated our model may appear at first glance, there are only three underlying principles involved in its construction:

A. The notion that endothelial cell migration is essentially a "diffusive" process based on the notion of reinforced random walks. An essential ingredient in this notion is the incorporation of transition probabilities which "reinforce" the walking. These transition probabilities are taken to be functionally dependent on the concentration of proteolytic enzymes which promote cell movement by degrading the ECM basement membrane and upon variations in the density of fibronectin in the vessel wall.
B. The proteolytic enzymes themselves are regarded as the products of a catalytic "reaction" of angiogenic factors with the cell of Michaelis-Menten type. The "catalyst" for this reaction is taken to be the receptor molecules which project from the cell interior through the cell wall and which bind to the angiogenic factor.

C. The enzyme, in its turn, acts as a catalyst for the degradation of the capillary basement membrane. (This process is well known to be governed by Michaelis-Menten kinetics.)

The analytical, biological and numerical consequences of the model include the following:

A. The computations indicate that the larger the transition probability sensitivity factors are, i.e., the more sensitive EC movement is to gradients in protease and in fibronectin, the more quickly they gather in the opening of the lumen which is created by the protease. Also, the size of the opening in the capillary wall is not much dependent on the variation in sensitivities. (Figure 14.)
B. The size of the opening in the lumen is dependent both on the gradients in growth factor along the capillary wall (Figure 10) and on the mean concentration of growth factor along the capillary wall. (Figures 13, 16.)
C. When sufficient angiogenic factor is supplied to the cell walls, either initially, or from a "remote" source, the breakdown of the basement lamina is concurrent with a bimodal distribution of endothelial cells. (Figures 6, 7, 11, 17.)
D. There is rapid conversion of growth factor into protease. (Figure 8.) (Consequently growth factor diffusion may be neglected in this model.)

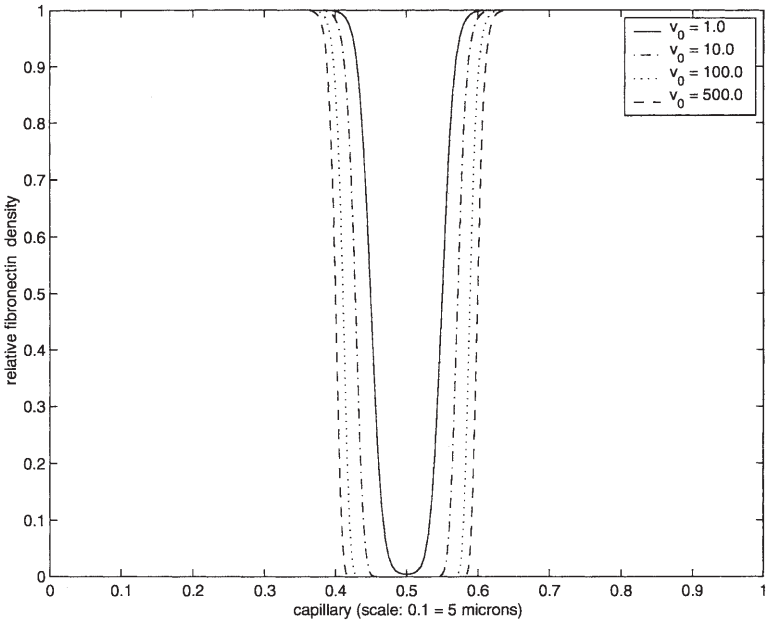

Fig. 16. Dependence of the opening on the initial dosage in $v(x, 0)$ (the parameter v_0) for (3.2)–(3.4). Fibronectin densities at $t = 0.2$ hours. As in Figure 13, as v_0 increases, the size of the opening increases.

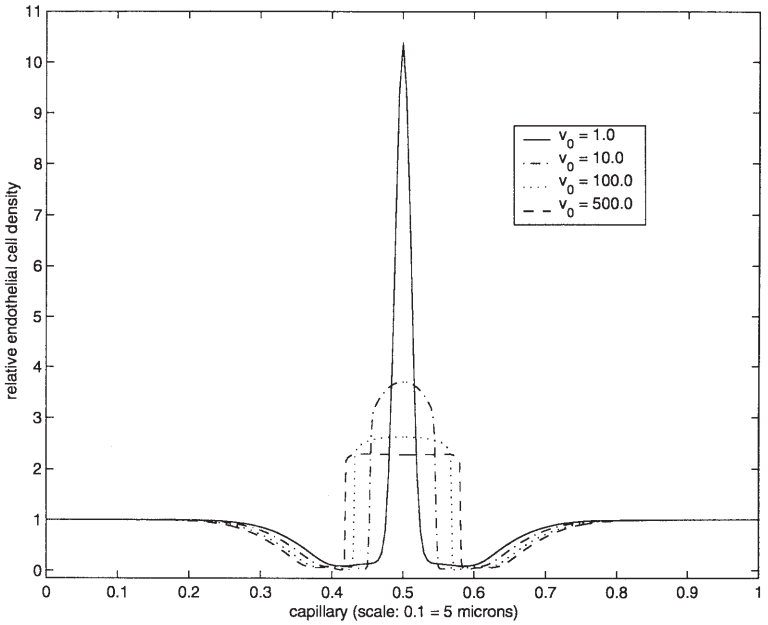

Fig. 17. Dependence of the opening on the initial dosage in $v(x, 0)$ (the parameter v_0) for (3.2)–(3.4). Endothelial cell densities at $t = 0.2$ hours. As in Figure 14, as v_0 increases, the EC distribution flattens and broadens.

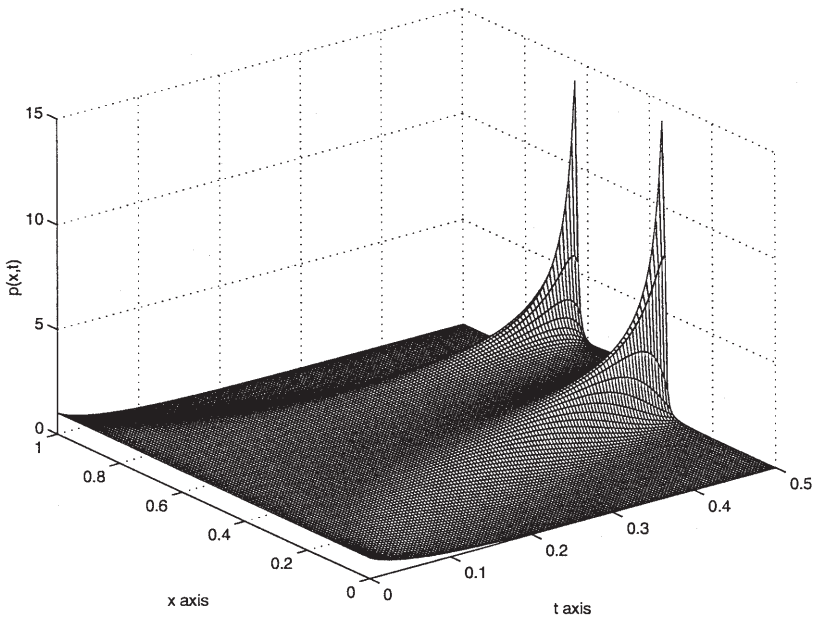

Fig. 18. These are plots for (7.4.1)–(7.4.2). As data constants, we took $D = 0.04$, $\gamma_2 = 10.0$, $\epsilon = 0.80$ and $m = 3.0$ (Figure P) Bimodal finite time blow up for $p(x, t)$.

E. When a protease decay term is included in the model, the model predicts that a small initial concentration of growth factor can lead to a permanent weakening of the capillary basement membrane. (Figure 21 and Section 7.5.)
F. The model possesses a number of unusual mathematical features:
    1. Depending on the size of the initial data, solutions (here, the endothelial cell density profiles) can exhibit characteristics of solutions of parabolic, elliptic or hyperbolic equations.
    2. This behavior is due to the fact that the system as a whole is *not* weakly parabolic, but rather has the property that it is a system with one variable (η) governed by an equation possessing infinite speed of propagation while the other variables are governed by equations possessing zero speed of propagation (c, v, f).

Finally, it should be remarked that bimodal distributions of epithelial cells occur in nature, for example during the fetal development of teats [4]. During the formation of mammary ducts, a sheet of epithelial cells on the surface of a fetus is subjected to a localized stimulus of growth factor from the fetal interior. This causes the epithelial cells to to aggregate at the surface around the stimulus site in a ring. The cells presumably emit a protease which breaks down the supporting surface. The cells form a small mound which then penetrates into the fetal interior when the supporting surface breaks down. This leads to the formation of the mammary duct at the site of the stimulus.

This roughly corresponds to what one might expect from a two dimensional version of our model. It is quite strong biological evidence for the "wave like" behavior of solutions of these equations.

In the same way, we propose that bimodal EC distribution may also be the precursor of the lining of a new endothelial cell wall for a sprouting capillary.

6. Current and future work

The processes involved in gaining a fuller understanding of angiogenesis is complex and not well understood. For example, we have not addressed the effects on our results if haptotactic saturation of fibronectin is taken into account as well as its production. Nor have we addressed the roles of the mast cells, macrophages and the pericytes. These aspects will be the subject of further work. In addition there is also the fundamental and far more daunting problem of linking the capillary sprout model to modeling angiogenesis within the ECM.

We wish to emphasize that this work is only a beginning attempt to model a very complex problem. However, we strongly believe that by carefully identifying the biological components of angiogenesis as well as by employing the ideas of reinforced random walk, we should be able to improve the current state of tumor modeling. (Together with our student, Serdal Pamuk, we have already coupled these equations to the analogous two dimensional model and obtained quite a good qualitative description of a capillary branching from a given capillary and lining itself with endothelial cells as it progresses across the ECM.)

Naturally, the more variables one introduces into the system, the more unwieldy it becomes. This is especially true when we attempt, as we are currently doing, to

couple the system in the capillary with the corresponding system in the ECM. As we see, the above system involves four differential equations. If we add angiostatin to the model, and assume that it acts by means of inhibiting proteolyic enzyme via a Michealis-Menten type mechanism of the type discussed above, then we add two more differential equations to the system, one for the consumption of angiostatin and one for the production of protease inhibitor. These two equations, together with an equilibrium equation between active and inactive inhibitor, quickly brings the number of equations to six differential and one algebraic equation in the capillary basement membrane. Correspondingly, there will be six transport equations and one more algebraic equations in the ECM and we are up to twelve differential equations, two algebraic equations and one coupling equation between the ECM dynamics and the basement membrane dynamics. Now consider cell movement equations for the macrophage cells and the pericyte cells and one of the pathways proposed by Folkman whereby TNF-α is transformed by macrophage cells to produce growth factor. When all is said and done, this pathway alone leads to a total of twenty two equations, all but two of which are differential equations. The conclusion of all of this is that biological processes are complicated and much more difficult to model problems in classical fluid dynamics, for example. However, we think our approach is one that should greatly aid in the understanding of angiogenesis and its regulation.

Currently, as we mentioned in the preceding paragraph, we have in progress a paper that incorporates introduces the macrophage cells and pericyte cells into this model. A further interesting feature of this model is the introduction of angiostatin as an inhibitor of angiogenesis. In this new model, we will take the point of view that angiostatin introduced into the bloodstream or produced in vivo binds with endothelial cells via receptors following a mechanism similar to the one introduced in this paper. It then produces an inhibitor which binds a significant portion of the enzyme, rendering it incapable of acting as a catalyst for the destruction of fibronectin.

Additionally, Professor Steven Ford and his students in the Department or Animal Science at Iowa State are designing chick embryo assays to help with the problem of getting better phenomenological constants for this problem. By doing a number of such assays, we should obtain sufficient data to determine values of these constants for real living systems, to at least reasonable orders of magnitude.

7. Appendix: Mathematical analysis of the system (2.2.22)–(2.2.23)

Here we explain various underlying mathematical features of the model which may be of interest to some readers. The appendix is divided into subsections which illustrate the rich mathematical content of the system (2.2.22).

1. Subsection 7.1. Capillary sprout formation and the onset of instability of the rest state.
2. Subsection 7.2. Elliptic properties of (2.2.22).
3. Subsection 7.3. Hyperbolic properties of (2.2.22).
4. Subsection 7.4. The onset of bimodal cell distribution.
5. Subsection 7.5. Parabolic properties of (2.2.22), protease decay and the existence of steady states.

We will work on $[0, \pi]$ throughout this Appendix.

7.1. Capillary sprout formation and the onset of instability of the rest state

In this section we consider the full system (2.2.22)–(2.2.23). We assume that the normalizations $\eta_0 = 1$ and $f_M = 1$ have been done. A steady state solution or a rest state for this system is a 4−tuple, $(\eta_s(x), c_s(x), v_s(x), f_s(x))$. Certainly trivial steady states exist. For example, any 4−tuple of the form (η_1, v_1, c_1, f_1) such that $(\beta(1-f_1)\eta_1 - c_1\gamma)f_1 = 0$ for which all the constants are nonnegative, is a steady state solution.

The rest point of interest here is $(1, 0, 0, 1)$. This is the normal state of a capillary with uniform endothelial cell density in the absence of angiogenic factor and proteolytic enzyme. Our goal in this section is to show that such rest points are initially unstable. However, this problem is *not* in the form of a standard nonlinear dynamical system. (Indeed, when we tried to prove stability or instability by perturbing $v(x, 0)$, we were only able to show marginal stability of the linear problem, a fact which says even less about the full problem than linear instability!)

The mathematical reason for this difficulty is that in a standard system of reaction-diffusion equations, even in those used to study chemotaxis, the dependent variables all possess the "infinite speed of propagation" principle normally associated with solutions of the heat equation. In this problem, only the dependent variable η possesses this property. The transport equations for v, c, f on the other hand, are ordinary differential equations and as such, the speed of propagation for these variables is zero.

Before going further, we should remark that we are not asserting the nonexistence of non constant steady states. However, we will give an argument to show that their existence is unlikely when protease decay is absent ($\mu = 0.$) (See Section 7.5 below.)

In order to elucidate further on the remarks of the preceding paragraph, we recall some of our results in [31] concerning the system namely

$$\begin{aligned} P_t &= D[P\ln(P/\tau(W))_x]_x \\ W_t &= WR(P, W) \\ P\ln(P/\tau(W))_x &= 0 \quad \text{at} \quad x = 0, \pi \\ P(x, 0) &= P_0(x) > 0 \\ W(x, 0) &= W_0(x) > 0 \end{aligned} \tag{7.1.1}$$

whose biological applications were discussed in [41] along with a detailed set of numerical experiments. The system was proposed there as a model for the study of fruiting bodies such as *Myxococcus fulvus* and *Dictyostelium discoideum* amoeba.

In [31], it was shown how, under various assumptions on $R(\cdot, \cdot)$, $\tau(\cdot)$ one could expect the phenomena of finite time blow up, infinite time collapse or even aggregation of solutions.

The underlying reason for these phenomena is contained in the fact the system (7.1.1) actually behaves, in the variable $\psi = \ln W$ like a quasi linear second

order partial differential equation with a strongly damped term (ψ_{xxt}).[11] The second order operator turns out to have the property that it will be elliptic for *small* initial values of ψ but it will be hyperbolic for *large* initial values of this variable.

The delicate nature of the system (7.1.1) carries over with a vengeance here as we shall argue in the following two sections. In this section we shall show that we can expect a short time instability (onset of instability) in the presence of a small initial quantity of proteolytic enzyme. To see this more clearly, we shall use the sensitivity factors (2.2.13). (This just simplifies the discussion. See the next section.)

We take our initial conditions in the form

$$\begin{aligned} \eta(x,0) &= \eta_0 = 1, \\ v(x,0) &= v_0 = 0, \\ c(x,0) &= c_0 = \epsilon\theta(x). \\ f(x,0) &= f_M = 1 > 0 \end{aligned} \tag{7.1.2}$$

where $\epsilon\theta > 0$ is some initial disturbance in enzyme concentration normalized in such a way that $\int_0^\pi \theta(x)\,dx = 1$.

It follows from local uniqueness that $\epsilon\theta(x) - c(x,t) = v(x,t) = 0$ on the existence interval.

Since f is close to unity for a short time, we have

$$f(x,t) \approx e^{-\lambda_2 \epsilon t \theta(x)}$$

and consequently

$$\eta_t = D\eta_{xx} - [(\gamma_1/\theta(x) + t\epsilon\lambda_2\gamma_2)\theta'(x)\eta]_x. \tag{7.1.3}$$

(We have dropped the tildes on the $\tilde{\gamma}_i$ here.) Suppose further that $\theta = 1 + \delta\phi$ for small δ so that $\int_0^\pi \phi(x)\,dx = 0$ and $\theta \geq 1 - \delta > 0$ on $[0,\pi]$. We assume also that θ and hence ϕ is unimodal, symmetric about $x = \pi/2$ and strictly increasing on $[0,\pi/2)$. We consider, instead of (7.1.3),

$$\eta_t = D\eta_{xx} - \Lambda(t)[\phi'(x)\eta)]_x \tag{7.1.4}$$

where

$$\Lambda(t) = \delta(\gamma_1 + \epsilon\lambda_2\gamma_2 t).$$

Thus, as long as f is close to unity, equation (7.1.4) tells us that η will tend to aggregate toward the point $x = \pi/2$. (One can most clearly see this in the extreme

[11] One can perhaps see the effect of this term easily by considering the problem $u_{tt} + u_{xx} - \epsilon^2 u_{xxt} = 0$ on $[0,\pi] \times [0,\infty)$ with $u_x = 0$ at $0, \pi$. Then the solution can be expanded in a cosine series. Given any $T > 0$ it is not hard to construct $u(x,0),\ u_t(x,0)$ such that the solution of this initial boundary value problem blows up in finite time when $\epsilon = 0$.) However, when $\epsilon > 0$, except for the constant first term, the terms will be of the form $a_n e^{\lambda_n t}$ where the sequence $\{\lambda_n\}_{n=1}^{+\infty}$ has least upper bound $2\epsilon^{-2}$. This means that instead of finite time blow up for this problem when $\epsilon = 0$ the solutions can grow no faster than $ce^{\epsilon^{-2}t}$. (This is a stabilizing mechanism for Hadamard's famous example of an improperly posed problem.)

case when $D = 0$ when (7.1.4) becomes first order. Then a characteristic in the (x, t)-plane beginning at $x = x_0$ to the left of $\pi/2$ will increase and have a vertical asymptote at $x_1(x_0) \leq \pi/2$. See also [55] for a discussion of problems of the form (7.1.4).

In this sense, then, we have shown that the rest state $(1, 0, 0, 1)$ is unstable, at least for short times.

Such an argument cannot be used to make any conclusions for long times. For example, if we perturb f initially instead of c, then $c(x, t) = v(x, t) = 0$ for as long as η is defined. Writing $f(x, 0) = 1 - \epsilon\theta(x)$ where ϵ is very small, then the equation that replaces (7.1.4) is

$$\eta_t = D\eta_{xx} - \epsilon\Lambda\left[\frac{\theta'(x)}{1 - \epsilon\theta(x)}\eta\right]_x \tag{7.1.5}$$

at least for small times where now $\Lambda = \lambda_2\gamma_2$. Again there is a tendency for η to aggregate near the center of the interval. Now, however, $f_t = \beta f(1 - f)\eta \geq 0$ so that f returns to its initial value, $f_M \equiv 1$, and consequently $\eta \to 1$.

7.2. Elliptic properties of (2.2.22)

If $v(x, 0) = \theta(x)$ and $c(x, 0) = 0$, then at least for as long as the solution exists, $c(x, t)+v(x, t) = \theta(x)$. We suppose that $\theta(x)$ is small so that $\lambda_2\theta/(1+\nu_2\theta) \approx \lambda_2\theta$.

In order to understand the elliptic nature of (2.2.22), we again consider a simplified version using the sensitivity factors (2.2.13) (with the γ_i replaced by $D\gamma_i$). We assume that c has come to a steady state, say $\theta(x)$ and that $v \equiv 0$. To see just how the resulting system exhibits elliptic (actually mixed type) behavior, we suppose that near equilibrium we are in a region in $x - t$ space where f is small. Then $1 - f(x, t) \approx 1$.

We then have the simplified system:

$$\begin{aligned} \eta_t &= D\eta_{xx} - D\left[\eta\left(\gamma_1\tfrac{\theta'(x)}{\theta(x)} - \gamma_2\tfrac{f_x}{f}\right)\right]_x \\ f_t &= (\beta\eta - \lambda_2\theta)f. \end{aligned} \tag{7.2.1}$$

This system bears a close resemblance to the system (7.1.1). To see this, we write $g = \ln f$. Then $g_t = \beta\eta - \lambda_2\theta$. After some manipulation, we see that $g(x, t)$ must satisfy

$$\mathfrak{L}g \equiv g_{tt} - D\gamma_2(g_t g_x)_x = Dg_{xxt} + G(g_x, g_t, \theta, \theta', \theta''). \tag{7.2.2}$$

The function G is linear in ∇g and vanishes as $\theta, \theta'/\theta, \theta'' \to 0$. The second order, quasi linear operator $\mathfrak{L}$ has discriminant

$$\mathfrak{D}(x, t) \equiv \mathfrak{D}(g_x(x, t), g_t(x, t)) = D\gamma_2(D\gamma_2 g_x^2 + 4g_t). \tag{7.2.3}$$

The operator $\mathfrak{L}$ will therefore be elliptic in those regions where $\eta < \lambda_2\theta(x)/\beta$ and where $\mathfrak{D}(x, t) < 0$, i.e. where η is small and f is small and fairly constant. On the other hand, if $\mathfrak{D}(x, t) > 0$, the operator will be hyperbolic. This will occur if $\eta > \lambda_2\theta/\beta$.

We can exploit these ideas somewhat further, by letting $\theta, \theta'/\theta, \theta'' \to 0$. The limiting equation that g must satisfy (after rescaling in t, g so that we can take $D = \gamma_2 = 1$) is

$$\mathfrak{Q}g \equiv g_{tt} - (g_t g_x)_x = g_{xxt} \tag{7.2.4}$$

where the boundary conditions reduce to $g_{xt} = g_t g_x$ at $x = 0, \pi$.

This problem has two exact solutions of interest here. They are

$$g_\pm(x,t) = \pm t \mp \ln[1 \pm 2\epsilon e^{2c_\pm t}\cos(2x) + \epsilon^2 e^{4c_\pm t}] \tag{7.2.5}$$

where $c_+ = 1/(1+\sqrt{2})$ and $c_- = -1$. The solution g_+ is such that $\partial_t g_+$ is negative (or $\eta < 0$). Moreover, both $g_+, \partial_t g_+$ blow up in finite time $c_+ T = \ln(1/\epsilon)$ *for every positive* ϵ. As $\epsilon \to 0^+$, $(g_+, \partial_t g_+)$ converges to $(-t, -1)$ although this convergence is *not* uniform in t. In terms of the discussion of the preceding paragraph, this corresponds to the case of "small η", that is $\eta < \lambda_2\theta/\beta$, the elliptic case, when $\theta > 0$). This blow up occurs on the so called "parabolic boundary", that is, on the point set where $\mathfrak{D}(x,t) = 0$. See [31] for details.

On the other hand, the solution g_- is such that $\partial_t g_-$ is positive (or $\eta > 0$). Moreover, as $t \to +\infty$, $g_-/t, \partial_t g_-$ converge uniformly to (1, 1) while as $\epsilon \to 0^+$, $(g_-, \partial_t g_-)$ converges uniformly to $(t, 1)$. In terms of the discussion of the preceding paragraph, this corresponds to the case of "large η," that is $\eta > \lambda_2\theta/\beta$, the hyperbolic case when $\theta > 0$).

The point of this is that in a certain sense, the single equation (7.2.4) is intrinsic to the system (2.2.22) and we can expect to understand the system by understanding the nature of the solutions of the initial-boundary value problem for (7.2.4). We shall return to this point later. For now, we note that when singularities form, we can expect that they form on the so-called parabolic boundary for (7.2.4). (We say "so called" because (7.2.4) is really a third order partial differential equation as remarked in above.)

7.3. Hyperbolic properties of (2.2.22)

The system (2.2.22) can perhaps also understood in the following way. In general, endothelial cell movement is quite slow while the cells themselves are fairly sensitive to changes in proteolytic enzyme and fibronectin. We interpret this as follows. If we set $D\gamma_i = \rho_i$, for $i = 1, 2$ and let $D \to 0$, $\gamma_i \to +\infty$ in such a way that ρ_i are fixed positive constants, then first equation in (2.2.22) takes the form:

$$\frac{\partial \eta}{\partial t} = -\frac{\partial(\Theta_x \eta)}{\partial x} \tag{7.3.1}$$

where

$$\Theta_x(x,t) \equiv \tilde{\chi_c} c_x + \tilde{\chi_f} f_x \tag{7.3.2}$$

where now $\tilde{\chi_c}$ and $\tilde{\chi_f}$ are independent of D and the γ_i. Notice that in view of the choices for the α_i, β_j, $\tilde{\chi_c} > 0$ and $\tilde{\chi_f} < 0$. (Here $\Theta = \ln\tau$ with γ_i replaced by ρ_i.)

While the function $\Theta(x,t)$ is itself dependent on η through the remainder of the equations (2.2.22), it is instructive to look at a simple version of (7.3.1) as though it

Table A

Interval	Sign of Θ_x	Sign of Θ_{xx}	Behavior of x	Behavior of N
$(0, b)$	$\Theta_x > 0$	$\Theta_{xx} > 0$	x increases	N decreases
$x = b$	$\Theta_x > 0$	$\Theta_{xx} = 0$	x increases	N is constant
(b, a)	$\Theta_x > 0$	$\Theta_{xx} < 0$	x increases	N increases
$x = a$	$\Theta_x = 0$	$\Theta_{xx} < 0$	x is constant	N increases
(a, c)	$\Theta_x > 0$	$\Theta_{xx} > 0$	x increases	N decreases
$x = c$	$\Theta_x < 0$	$\Theta_{xx} = 0$	x decreases	N is constant
$(c, +\infty)$	$\Theta_x < 0$	$\Theta_{xx} < 0$	x decreases	N increases

were a known function. Given the forms that f and c appear to take as time evolves (as we see in the numerical examples below) it is possible to make some qualitative statements about the behavior of η.

To do this we consider the initial value problem for (7.3.1) with Θ a symmetric bimodal function of x alone. (For example, $\Theta(x) = x^2(1 - x^2)$.) We assume that Θ has two relative maxima at $x = \pm a$ and a minimum at $x = 0$. We also assume that Θ has two inflection points at $\pm b$ and $\pm c$ with $b < a < c$. Then with $N = \ln \eta$ we can rewrite (7.3.1) in the form

$$N_t + \Theta_x N_x = -\Theta_{xx}. \tag{7.3.3}$$

From this and the characteristic equations, we glean the following information for the behavior of x and N along the characteristics with increasing characteristic parameter t:

For $x < 0$ we obtain a similar table.

We conclude: *Under the above assumptions on* Θ, *the solutions of (7.3.1) will aggregate at the points where* Θ *is a maximum and de-aggregate (collapse) at the points where* Θ *is a minimum.* In this example, we expect collapse at $x = 0, \pm\infty$ and blow up at $x = \pm a$.

However, when there is diffusion present, i.e.,

$$\eta_t + \Theta_x \eta_x = \epsilon \eta_{xx} - \Theta_{xx} \eta \tag{7.3.4}$$

where now ϵ is a small, positive constant, it is possible that as the gradients in η_x become large, the maxima may coalesce to a single maximum as time evolves or only a single maximum may appear as time evolves with or without single point blow up. A third possibility is that one has finite or infinite time blow up at two points before the maxima have had a chance to coalesce to a single point. Finally, there is the possibility that one obtains a bimodal steady state.

It is important to keep in mind, in the computations below, that the function $\Theta(\cdot, \cdot)$ is dependent on the initial values of our dependent variables, to say nothing of its dependence upon the various constants in our system. That is, we may exaggerate the drift term $\partial_x(\eta\Theta_x)$ at the expense of the diffusion term, $\epsilon\eta_{xx}$ in several ways other than by letting $\epsilon \to 0$. For example, by the simple expedient of increasing the gradient and magnitude of the initial concentration of TAF or the rate of input of this chemical, we can force Θ to have larger gradients in x.

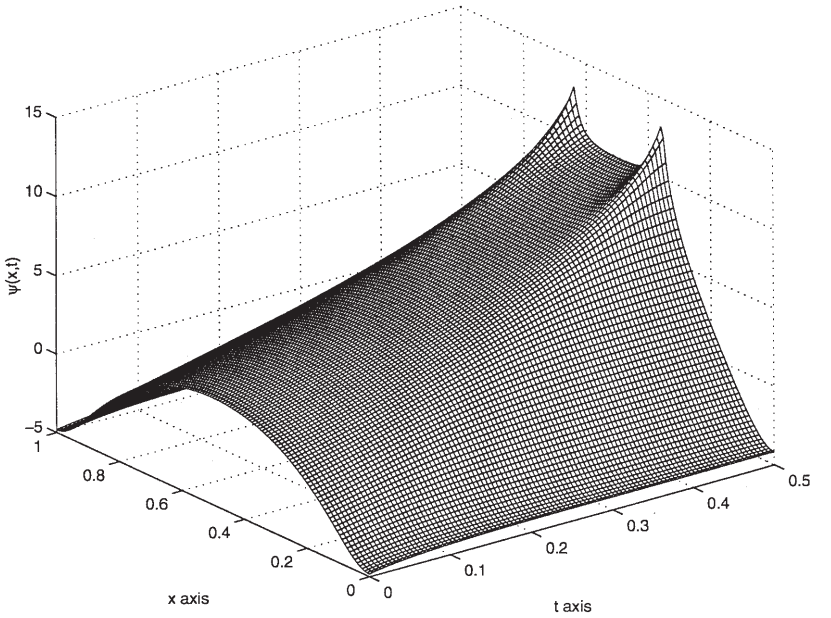

Fig. 19. These are plots for (7.4.1)–(7.4.2). As data constants, we took $D = 0.04$, $\gamma_2 = 10.0$, $\epsilon = 0.80$ and $m = 3.0$ (Figure W) Bimodal finite time blow up for $w(x, t)$.

7.4. The onset of bimodal cell distribution

One question to be answered that arises naturally from the above discussion is the following: If we start with a unimodal distribution in $v(x, 0)$ or $v_r(x, t)$ can a bimodal distribution in $\ln(\tau)$ develop? This turns out to be a rather non trivial question. Moreover, the figures below show that, especially when the gradients $\partial_x v(x, 0)$ or $\partial_x v_r(x, t)$ are large, this does happen. The bimodal structure of $\ln(\tau)$ in turn leads to the biomodality of η, the EC distribution and provides evidence that our model is in agreement with biology since the bimodal EC distribution corresponds to the beginnings of the EC lining of the nascent capillary.

In order to explain more fully how this bimodal distribution can arise, let us appeal once more to an alternate form of (7.2.4). We consider, as in [31] the problem:

$$\begin{aligned} p_t &= D(p_{xx} - \gamma_2(\psi_x p)_x) \\ \psi_t &= p \end{aligned} \tag{7.4.1}$$

on $(0, \pi)$ for $t > 0$. (Here we make the identifications $\psi = -g$ and $p = \lambda_2\theta - \beta\eta$ and assume θ is constant.) We take $p_x = 0$ at $x = 0, \pi$. In [31,41] the initial conditions were $p(x, 0) = 1 - \epsilon\cos(2x)$ and $\psi(x, 0) = \ln w(x, 0) = 0$. In [31] the computations of [41] were repeated to show that the single point blow up p was of the same form as for g_t discussed above and that the numerical evidence indicated that this solution blows up on the parabolic boundary, i.e. where $\mathfrak{D}(x, t) \equiv (\gamma_2 D)^2\psi_x^2 - 4(\gamma_2 D)\psi_t = 0$. The initial data are such that initially $\mathfrak{D}(x, 0) < 0$, i.e., the solution begins in the so called "elliptic region" of the pseu-

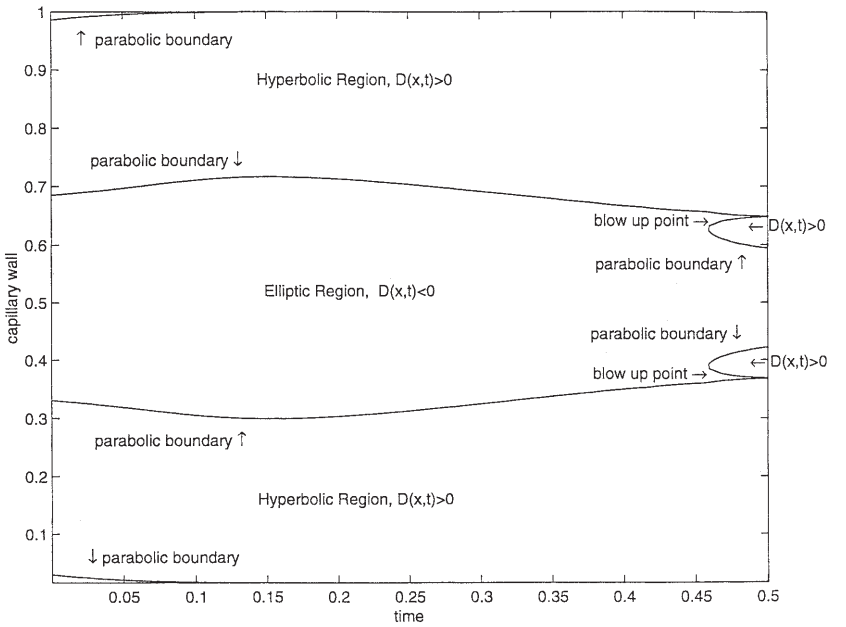

Fig. 20. These are plots for (7.4.1)–(7.4.2). As data constants, we took $D = 0.04$, $\gamma_2 = 10.0$, $\epsilon = 0.80$ and $m = 3.0$ (Figure C) Contour plot for the discriminant $\mathfrak{D}(x, t)$. Regions of ellipticity and hyperbolicity.

do hodograph plane and traces out a vertical segment in the (ψ_x, ψ_t) (hodograph) plane. Instead, this time we take initial data:

$$\begin{aligned} \psi(x, 0) &= m \ln(1 - \epsilon \cos(2x)), \\ \psi_t(x, 0) &= p(x, 0) = 1. \end{aligned} \tag{7.4.2}$$

We now find

$$\mathfrak{D}(x, 0) = 4\gamma_2 D\left(\frac{\gamma_2 D m^2 \epsilon^2 \sin^2(2x)}{(1 - \epsilon \cos(2x))^2} - 1\right)$$

a quantity that changes sign.[12] (Indeed, it is negative at the center and ends of the interval and will be positive at $x = \frac{\pi}{4}, \frac{3\pi}{4}$ if $m^2\epsilon^2 D\gamma_2 > 1$. This means that our solution will initially be partially in the elliptic region and partially in the hyperbolic region. We then expect single point blow up on each of the two curves emanating from the $x-$axis for which $\mathfrak{D}(x, t) = 0$ which form the boundary of the central elliptic region. In Figures 18–20, we have plotted p, ψ and the regions in the $x - t$ plane where (7.4.2) is elliptic, and where it is hyperbolic (and reverted to the interval $[0, 1]$). Notice that in Figure 20 of this set, the finite time, bimodal blow up occurs precisely on the parabolic boundary. Notice also that although ψ is unimodal, it (as well as does p) develop a bimodal distribution as per the opening paragraph of this subsection.

[12] In terms of the original variables, $f(x, 0) = (1 - \epsilon \cos(2x))^{-m}$ and $\eta(x, 0) = (\lambda_2\theta - 1)/\beta$.

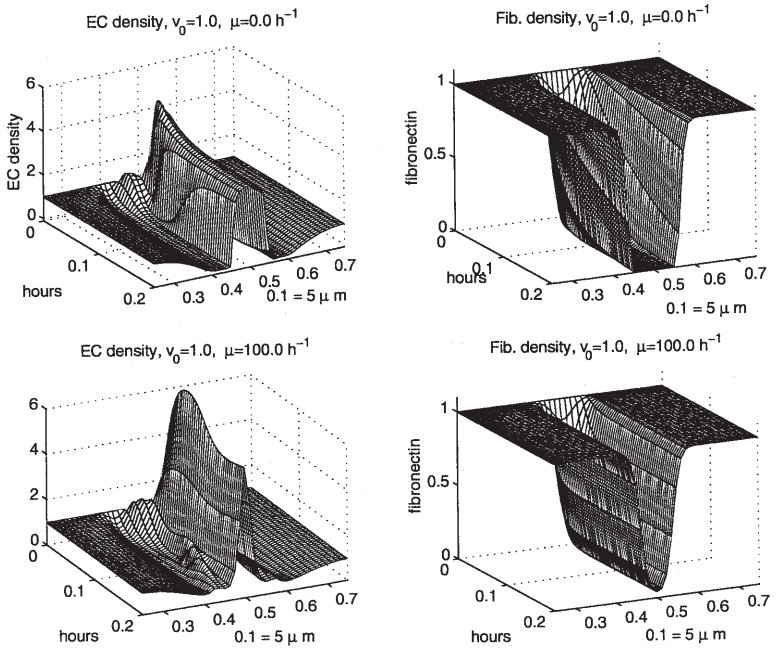

Fig. 21. The top row of figures illustrates the time evolution when $\mu = 0$ or no protease decay is present in the model. The second row of figures illustrates the time evolution when $\mu = 100\ h^{-1}$. In both cases, $m = 100$. See the discussion in Section 7.5.

This computation suggests (but does not prove) that an initial unimodal distribution in f together with an initial constant distribution in η can give rise to a bimodal distribution in η.

Notice here that as m becomes large, the initial channel in f becomes narrower and the hyperbolic interval becomes larger while the elliptic region becomes narrower. Thus we expect the two peaks to coalesce as the channel narrows.

7.5. Parabolic properties of (2.2.22) and the role of protease decay in the existence of steady states

If the system (2.2.22) exhibits properties we normally associate with hyperbolic equations and properties we normally associate with elliptic equations, it seems reasonable to ask if it can ever exhibit properties we normally associate with parabolic equations. For example, are there non constant, stable steady states?

To see how we might try to find non constant steady states for (2.2.22), we consider a steady state that could arise from a perturbation of the initial data for (2.2.22) in the form:

$$\begin{aligned} \eta(x,0) &= 1 \\ v(x,0) &= \epsilon\theta(x) \\ c(x,0) &= 0 \\ f(x,0) &= 1. \end{aligned} \tag{7.5.1}$$

Correspondingly let us write

$$\begin{aligned} \eta(x,t) &= 1 + \epsilon N(x,t,\epsilon) \\ v(x,t) &= \epsilon w(x,t,\epsilon) \\ c(x,t) &= \epsilon \xi(x,t,\epsilon) \\ f(x,t) &= 1 - \epsilon \phi(x,t,\epsilon). \end{aligned} \tag{7.5.2}$$

We let $\eta_s, N_s, v_s, w_s, c_s, \xi_s, f_s, \phi_s$ be the corresponding (ϵ dependent) stationary solutions, assuming they exist. We suppose also that these functions are at least twice continuously differentiable.

It is clear from the stationary equation for η that if η_s vanishes at a single point in $(0, \pi)$ then it must vanish on the entire interval. Moreover, from the comments in Section 7.2, it is reasonable to assume that $f_s(x) > 0$ throughout the interval $[0, \pi]$. More precisely, we assume that for such a solution

$$\lim_{t \to +\infty} \eta(x,t) = \eta_s(x) \geq \eta_{min} > 0. \tag{7.5.3}$$

From the second and third equations of (2.2.22) v_t is negative and c_t is positive but $c + v = \epsilon\theta$. Therefore, it is reasonable to take

$$\begin{aligned} w_s(x,\epsilon) &= 0 \\ \xi_s(x,\epsilon) &= \theta(x) \end{aligned}$$

and consequently

$$\phi_s(x,\epsilon) = \frac{\lambda_2 \theta(x)}{\beta(1 + \epsilon N_s(x,\epsilon))}. \tag{7.5.4}$$

After a quadrature, and using the boundary conditions for η_s we see that

$$\begin{aligned} N_s'(x,\epsilon) = (1 + \epsilon N_s(x,\epsilon)) \\ \times \frac{\partial_c \tau(\epsilon\theta(x), 1 - \epsilon\phi_s(x,\epsilon))\theta'(x) - \partial_f \tau(\epsilon\theta(x), 1 - \epsilon\phi_s(x,\epsilon))\phi_s'(x,\epsilon)}{\tau(\epsilon\theta(x), 1 - \epsilon\phi_s(x,\epsilon))}. \end{aligned} \tag{7.5.5}$$

Now (7.5.4), (7.5.5) constitute a pair of nonlinear equations in N_s, ϕ_s. In order to solve them for small ϵ, we first solve them for $\epsilon = 0$.

$$\begin{aligned} \phi_s(x,0) &= \frac{\lambda_2 \theta(x)}{\beta}, \\ N_s'(x,0) &= \frac{\partial_c \tau(0,1))\theta'(x) - \partial_f \tau(0,1)\phi_s'(x,0)}{\tau(0,1)}. \end{aligned} \tag{7.5.6}$$

Thus, we may integrate the second of (7.5.6) after eliminating $\phi_s(x,0)$ using the first of these. We obtain

$$N_s(x,0) = \Lambda(\theta(x) - 1) \tag{7.5.7}$$

where we have evaluated the constant of integration using $\int_0^\pi \eta(x,t)\,dx = \pi$, and where

$$\Lambda = \frac{\beta\partial_c\tau(0,1) - \lambda_2\partial_f\tau(0,1)}{\beta\tau(0,1)} \tag{7.5.8}$$

. Notice that, in view of the choice of the sensitivity constants, $\partial_f\tau(c,f) < 0$ so that both terms in the numerators of (7.5.5), (7.5.6) and (7.5.8) will be positive.

Thus, for ϵ small one might expect that

$$\begin{aligned}\eta_s(x,\epsilon) &\approx 1 + \epsilon\Lambda(\theta(x) - 1),\\ f_s(x,\epsilon) &\approx 1 - \frac{\epsilon\lambda_2\theta(x)}{\beta(1+\epsilon\Lambda(\theta(x)-1))}.\end{aligned} \tag{7.5.9}$$

However, this is only correct to first order in ϵ. The higher order (in ϵ) terms must also be included if the perturbation scheme is not regular.

That this may in fact be the case can be seen by considering the case $\epsilon > 0$ from the start.

Differentiating (7.5.4) we obtain

$$\phi_s'(x,\epsilon) = \left[\frac{\lambda_2\theta(x)}{\beta(1+\epsilon N_s(x,\epsilon))}\right]\left[\frac{\theta'(x)}{\theta(x)} - \frac{\epsilon N_s'(x,\epsilon)}{(1+\epsilon N_s(x,\epsilon))}\right]. \tag{7.5.10}$$

After a quadrature, and using the boundary conditions for η_s we see that

$$\begin{aligned}&\left[1 + \frac{\partial_f\tau(\epsilon\theta(x), 1-\epsilon\phi_s(x,\epsilon))}{\tau(\epsilon\theta(x), 1-\epsilon\phi_s(x,\epsilon))}\frac{\epsilon\phi_s(x,\epsilon)}{(1+\epsilon N_s(x,\epsilon))}\right]N_s'(x,\epsilon)\\ &\quad = (1+\epsilon N_s(x,\epsilon))\frac{\partial_c\tau(\epsilon\theta(x), 1-\epsilon\phi_s(x,\epsilon))\theta'(x)}{\tau(\epsilon\theta(x), 1-\epsilon\phi_s(x,\epsilon))}.\end{aligned} \tag{7.5.11}$$

One can then use (7.5.4) to eliminate $\phi_s(x,\epsilon)$ and solve the resulting ordinary differential equation as before. However, now one has to worry about the coefficient of $N_s'(x,\epsilon)$ which may vanish since

$$\partial_f\tau(\epsilon\theta(x), 1-\epsilon\phi_s(x,\epsilon))$$

is negative. If this coefficient vanishes at a point x for which $\theta'(x) \neq 0$ then N_s' will be undefined and the solution will not exist.

Numerical computations with $\epsilon = v_0$ show that this is precisely what happens. That is, computations indicate that $c(x,t)$ approaches a steady state while $\max_{x\in[0,1]}\{\eta(x,t)\}$ becomes unbounded but $\eta_{min}(t)$ (the quantity $(\min_{x\in[0,1]}\{\eta(x,t)\})$ approaches zero as t becomes large. Moreover, we see from Figures 11, 14 and 15 that η_{min} at $t = 0.2$ becomes smaller as we (a) increase v_0, m and the sensitivity powers γ_i.

On the other hand, when protease decay is included in the model, steady states appear to be possible. For example, in Figure 21, we compare the behavior of the solutions of the initial value problem when $v_0 = 1, m = 100$ in the two cases $\mu = 0$ (no protease decay) and $\mu = 100\ h^{-1}$ (protease decay.) The top row corresponds to the former case while the lower row of figures corresponds to the latter case.

The number μ we have chosen here is representative of *in vitro* decay constants we found in the literature for a selection of proteases.

Unfortunately, as we remarked earlier, these values can be quite different *in vivo*. The constants depend on temperature, pH and the other proteins in the local environment.

References

1. Adair, T.H., Gray, W.J., Montani, J.: New Paradigms for collateral vessel growth. Am. J. Physical, **259**, R393–R404 (1990)
2. Anderson, A.R.A., Chaplain, M.A.J.: A mathematical model for capillary network formation in the absence of endothelial cell proliferation Appl. Math. Lett., **11**, 109–116 (1998)
3. Anderson, A.R.A., Chaplain, M.A.J.: Continuous and discrete mathematical models of tumour induced angiogenesis, Bull. Math. Biology, **60**, 857–899 (1998)
4. Anderson, R.: Mammary gland, in Lactation, Bruce Larson, Editor, Iowa State University Press, Ames, 1–38 (1985)
5. Ausprunk, D.H., Folkman, J.: Migration and Proliferation of endothelial cells in preformed and newly formed blood vessels during tumor angiogenesis. Microvasc Re., **14**, 73–65 (1977)
6. Ankoma-Sey, V., Matli, M., Chang, K.B., Lalazar, A., Donner, D.B., Wong, L., Warren, R.S., Friedman, S.L.: Coordinated induction of VEGF receptors in mesenchymal cell types during rat hepatic wound healing, Oncogene, **17**, 115–121 (1998)
7. Batra, S., Rakusan, K.: Capillary network geometry during postnatal growth in rat hearts Am. J. Physiology. **262**, 635–640 (1992)
8. Bourdoulous, S., Orend, G., Mackenna, D.A., Pasqualini, R., Rouslahti, E.: Fibronectin matrix regulates activation of RHO and CDC42 GTPases and cell cycle progression, J. Cell. Biol., **143** (1), 267–276 (1998)
9. Batra, S., Rakusan, K.: Geometry of the vascular system-Evidence for a metabolic hypothesis, Microvasc, Res. **41**, 39–50 (1991)
10. Bowersox, J.C., Sorgente, N.: Chemotaxis of aortic endothelial cells in response to fibronectin Cancer Res. **4**, 2547–2551 (1982)
11. Chaplain, M.A.J., Stuart, A.M.: A model mechanism for the chemotactic response of endothelial cells to tumor angiogenesis factor, I.M.A. J. Math. Appl. Math. Biol., **10**, 149–168 (1993)
12. Chaplain, M.A.J., Giles, S.M., Sleeman, B.D., Jarvis, R.J.: A mathematical model for tumour angiogenesis, J. Math. Biol., **33**, 744–770 (1995)
13. Davis, B.: Reinforced random walks, Probal. Theory Related Fields, **84**, 203–229 (1990)
14. Dekker, A., Poot, A.A., van Mourik, J.A., Workel, M.P., Beugeling, T., Bantjes, A., Feijen, J., van Aken, W.G.: Improved adhesion and proliferation of human endothelial cells on polyethylene precoated with monoclonal antibodies directed against cell membrane antigens and extracellular matrix proteins, Thromb. Haemost., **66**(6), 715–724 (1991)
15. Engelmann, G.L., Dionne, C.A., Jaye, M.C.: Acidic fibroblast growth factor, heart development and capillary angiogenesis, Ann NY Acad. Sci. **638**, 463–466 (1991)
16. Fields, G., Netzewl-Arnett, S.J., Windsor, L.J., Engler, J.A., Berkedal-Hansen, H., van Wart, H.E.: Proteolytic activities of human fibroblast collagenaise; Hydrolysis of a broad range of substrates at a single active site Biochemistry, **29**, 6600–6677 (1990)
17. Englemann, G.L., Dionne, C.A., Jaye, M.C.: Acidic fibroblast growth factor and heart development – role in myocyte proliferation and capillary angiogenesis, Circ. Res., **72**, 7–19 (1993)

18. Folkman, J.: Angiogenesis-Retrospect and and outlook: in Angiogenesis: Key Principles-Science-Technology-Medicine, Steiner, R. Weisz, P.B. and Langer, R., Birhäuser, Basel, 1992
19. Folkman, J., Shing, Y.: Angiogenesis, J. Biol. Chem., **267**, 10931–10934 (1992)
20. Gordon, S.R., DeMoss, J.: Exposure to lysosomotropic amines and protease inhibitors retard corneal endothelial cell migration along the natural basement membrane during wound repair, Exp. Cell. Res., **246**(1), 233–242 (1999)
21. Gamble, J.R., Matthias, L.J., Meyer, G., Kaur, P., Russ, G., Faull, R., Berndt, M.C., Vadas, M.A.: Regulation of in vitro capillary tube formation by anti-integrin antibodies. J. Cell. Biol., **121**(4), 931–943 (1993)
22. Hudlicka, O., Brown, M., Egginton, S.: Angiogenesis in skeletal and cardiac muscle, Physical Rev, **72**, 369–417 (1992)
23. Hudlicka, O.: What makes blood vessels grow, J. Physical, **444**, 1–24 (1991)
24. Hudlica, O., Tyler, K.R.: Angiogenesis, Academic Press, London, (1986)
25. Kabelic, T., Ganbisa, S., Glaser, B., Liotta, L.A.: Basement membrane collagen: degradation by migrating endothelial cells. Science **221**, 281–283 (1983)
26. Klagsbrun, M.: Regulators of angiogenesis, Ann. Rev. Physical, **53**, 217–239 (1991)
27. Klagsburn, M., Folkman, J.: Angiogenesis in peptide growth factors and their receptors. Sporn, M.B. and Roberts, A.B., Eds., 549–586, Springer-Verlag, Berlin, (1990)
28. Kendall, R.L., Rutledge, R.Z., Mao, X., Tebben, A.J., Hungate, R.W., Thomas, K.A.: Vascular endothelial growth factor receptor KDR tyrosine kinase activity is increased by autophosporilazion of two activation loop tyrosine residues, J. Biol. Chem., **274**, 6453–6460 (1999)
29. Kuwano, M., Ushiro, S., Ryuto, M., Samoto, K., Izumi, H., Ito, K., Abe, T., Nakamura, T., Ono, M., Kohno, K.: Regulation of angiogenesis by growth factors, GANN Monograph on Cancer Research, **42**, 113–125 (1994)
30. Levine, H.A., Pamuk, S., Sleeman, B.D., Nilsen-Hamilton, M.: Mathematical Modeling of Capillary Formation and Development in Tumor Angiogenesis, manuscript
31. Levine, H.A., Sleeman, B.D.: A system of reaction diffusion equations arising in the theory of reinforced random walks, SLAM J. Appl. Math., **57**, 683–730 (1997)
32. Levine, H.A., Sleeman, B.D., Nilsen-Hamilton, M.: A Mathematical Model for the Roles of Pericytes and Macrophages in the onset of Angiogenesis I. The role of Protease Inhibitors in preventing Angiogenesis, Math. Biosciences (in press)
33. Morimoto, K., Mishima, H., Nishida, T., Otori, T.: Role of urokinase type plasminogen activator (u-PA) in corneal epithelial migration Thromb. Haemost., **69**(4), 387–391 (1993)
34. Murray, J.D.: Mathematical Biology, Biomathematics Texts, Springer-Verlag, (1989)
35. Nicosia, R.F., Bonanno, E., Smith, M.: Fibronectin promotes the elongation of microvessels during angiogenesis in vitro, J. Cell Physiol., **154**(3), 654–661 (1993)
36. Nerem, R.M., Levesque, M.J., Cornhill, J.F.: Vascular endothelial cell morphology as an indicator of the pattern of blood flow, J. Biomech. Eng., **103**(3), 172–176 (1981)
37. Nimono, H.R., Sleeman, B.D.: Fluid transport in vascularized tumors and metastasis, I.M.A. – J. Math Appl. Med. Biol., **15**, 73–98 (1998)
38. Olsen, L., Sherratt, J.A., Maini, P.K., Arnold, F.: A mathematical model for the capillary endothelial cell extra cellular matrix interactions in wound-healing angiogenesis. I.M.A. – J. Maths Applied in Med. and Biology, **14**, 261–281 (1997)
39. Orme, M.E., Chaplain, M.A.J.: A mathematical model of the first steps of tumour related angiogenesis: Capillary Sprout Formation and Secondary Branching. I.M.A. – Journal of Mathematics Appl. in Med. and Biol., **13**, 73–98 (1996)

40. Orme, M.E., Chaplain, M.A.J.: A mathematical model of the first steps of tumour related angiogenesis: Capillary sprout formation and secondary branching, I.M.A. – J. Math. Appl. Med. Biol., **13**, 73–98 (1996)
41. Othmer, H.G., Stevens, A.: Aggregation, blow up and collapse: The ABC's of taxis and reinforced random walks. SIAM J. Appl. Math., **51**, 1044– 1081 (1997)
42. Ostadal, B., Schiebler, T.H., Rychter, Z.: Relations between development of the capillary wall and myoarchitecture of the rat heart, Adv. Exp. Hed. Biol., **53**, 375–388 (1975)
43. Paweletz, N., Knierim, M.: Tumor related angiogenesis. Crit. Rev. Oncal. Hematol. **9**, 197–242 (1989)
44. Rakusan, K.: Development of cardiac vasculature. In Handbook of Human Growth and Developmental Biology, III/B. E. Meisami and P.S. Tuminas Eds., 101–106
45. Rakusan, K.: Cardiac growth, maturation and aging in growth of the heart in Health Disease, R. Zak (Ed.), 131–164, Raven Press New York (1984)
46. Rakusan, K.: Coronary Angiogenesis. From morphology to molecular biology and back Ann. NY Acad. Sciences, **752**, 257–266 (1995)
47. Rakusan, K., Turek, Z.: Protamine inhibits capillary formation in growing rat hearts, Circ. Res. **37**, 393–399 (1985)
48. Roberts, J.M., Forrester, J.V.: Factors affecting the migration and growth of endothelial cells from microvessels of bovine retina. Exp. Eye Res., **50**(2), 165–172 (1990)
49. Schaper, W.: New paradigms for collateral vessel growth, Basic Res. Cardial, **88**, 193–198 (1993)
50. Schott, R.J., Morrow, L.A.: Growth factors and angiogenesis. Cardiovasc, Res., **27**, 1155–1161 (1993)
51. Schleef, R.R., Birdwell, C.R.: The effect of proteases on endothelial cell migration in vitro Exp. Cell Res., **141**(2), 503–508 (1982)
52. Sherrat, J.A., Murray, J.D.: Models of epidermal wound healing, Proc. R. Soc. Lond. B, **241**, 19–26, (1990)
53. Sleeman, B.D.: Solid tumor growth: A case study in mathematical biology, Nonlin. Math. Appl., Ed. P.J. Aston, C.U.P., 237–256 (1996)
54. Sleeman, B.D.: Mathematical modelling of tumor growth and angiogenesis, Adv. in Exp. Med. Bio., **428**, 671–677 (1997)
55. Sleeman, B.D., Anderson, A.R.A., Chaplain, M.A.I.: A mathematical analysis of a model for capillary network formation in the absence of endothelial cell proliferation, Appl. Math. Let., **126**, 121–127 (1999)
56. Soldi, R., Mitola, S., Strasly, M., Defilippi, P., Tarone, G., Bussolino, F.: Role of alphavbeta3 integrin in the activation of vascular endothelial growth factor receptor-2, EMBO J., **18**(4), 882–892 (1999)
57. Turek, A., Hoofd, L., Rakusan, K.: Myocardial capillaries and tissue oxygenation. Can. J. Candiol, **2**, 98–103 (1986)
58. Turning, A.M.: The chemical basis of morphogenesis. Phil Trans. Roy. Soc. Lond B, **237**, 37–72 (1952)
59. Waltenberger, J., Claesson-Welsh, L., Siegbahn, A., Shibuya, M., Heldin, C-H.: Different signal transduction properties of KDR and Flt1, two receptors for vascular endothelial cell growth factor, J. Biolog. Chem., **269**, 26988–26995 (1994)
60. Yamada, K.M., Olden, K.: Fibronectins-adhesive glycoproteins of cell surface and blood Nature. **275**, 179–184 (1978)